

Derivation and Empirical Validation of a Refined Traffic Flow Model

Dirk Helbing

II. Institute of Theoretical Physics

University of Stuttgart

70550 Stuttgart

Germany

Abstract

The gas-kinetic foundation of fluid-dynamic traffic equations suggested in previous papers [Physica A **219**, 375 and 391] is further refined by applying the theory of dense gases and granular materials to the Boltzmann-like traffic model by Paveri-Fontana. It is shown that, despite the phenomenologically similar behavior of ordinary and granular fluids, the relations for these cannot directly be transferred to vehicular traffic. The dissipative and anisotropic interactions of vehicles as well as their velocity-dependent space requirements lead to a considerably different structure of the macroscopic traffic equations, also in comparison with the previously suggested traffic flow models. As a consequence, the instability mechanisms of emergent density waves are different. Crucial assumptions are validated by empirical traffic data and essential results are illustrated by figures.

PACS numbers: 47.50.+d,51.10.+y,47.55.-t,89.40.+k

Key Words: Kinetic gas theory, macroscopic traffic models, traffic instability, dense nonuniform gases, granular flow

1 Introduction

Modelling of traffic flow on highways presently attracts a rapidly growing community of physicists. Recent research focusses on microsimulation models [1] as well as on fluid-dynamic Navier-Stokes-like models [2, 3, 4, 5] and their derivation from the “microscopic” behavior of driver-vehicle units via gas-kinetic equations [6, 7]. Of particular interest is the description of traffic instabilities (cf. Fig. 1) which lead to the emergence of stop-and-go traffic above a certain critical vehicle density. This phenomenon is illustrated by Figure 2.

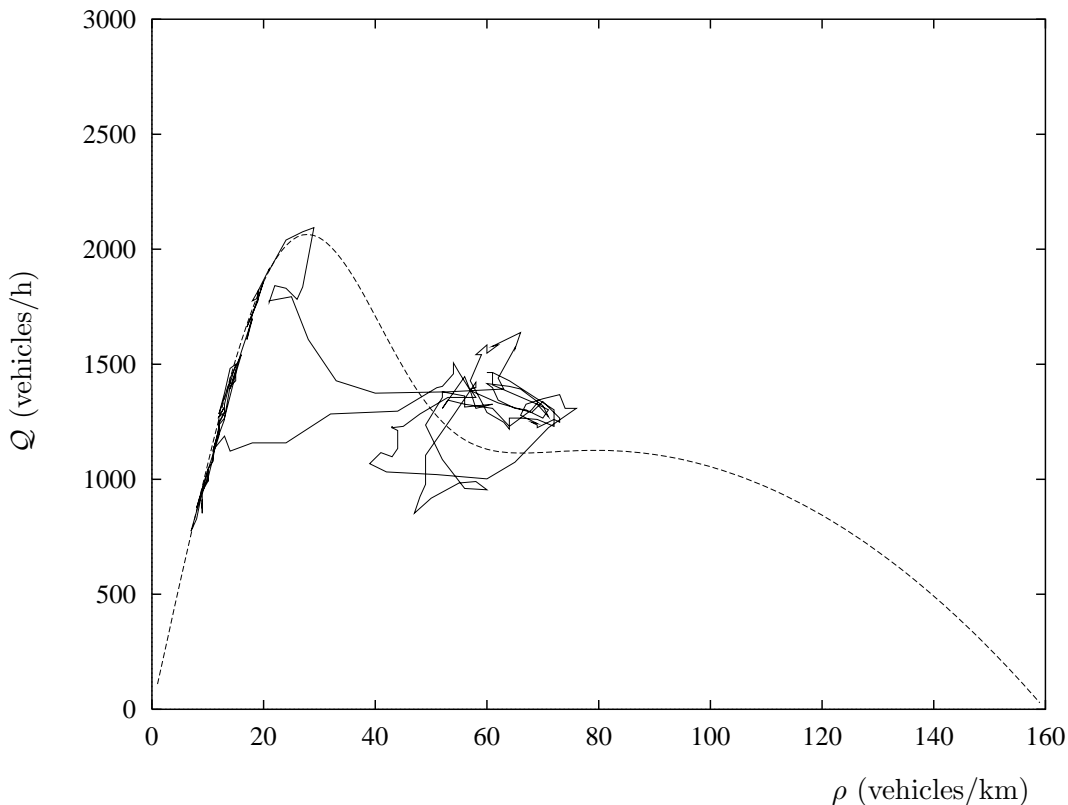


Figure 1: Illustration of the *fundamental diagram* $\mathcal{Q}(\rho) = \rho V_e(\rho)$ describing the equilibrium flow-density relationship (—) and of the temporal course $\mathcal{Q}(r, t) = \rho(r, t)V(r, t)$ of the empirical flow (—). Obviously, the equilibrium relation $\mathcal{Q}(r, t) = \mathcal{Q}_e(\rho(r, t))$ is only fulfilled at small densities. After the maximum flow is reached, the temporal development of the flow $\mathcal{Q}(r, t)$ shows the typical hysteresis phenomenon discovered by Hall [8] which indicates a phase transition from almost homogeneous flow to stop-and-go traffic. (Empirical data: Cross-section $r = 41.8$ km of the Dutch two-lane highway A9 from Haarlem to Amsterdam at November 2, 1994, between 6:30 am and 10:00 am.)

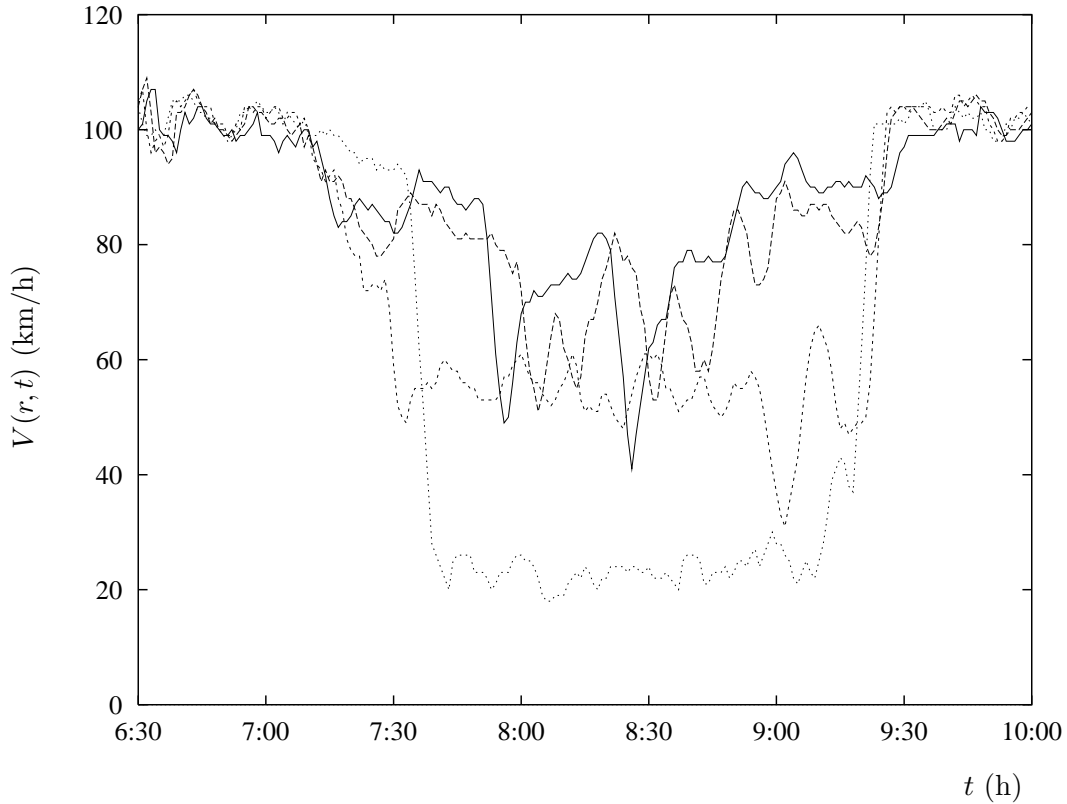


Figure 2: Temporal evolution of the mean velocity $V(r, t)$ at subsequent cross-sections of the Dutch highway A9 from Haarlem to Amsterdam at October 14, 1994 (five minute averages of single vehicle data). The prescribed speed limit is 120 km/h. We observe a breakdown of velocity during the rush hours between 7:30 am and 9:30 am due to the overloading of the highway at $r = r_0 := 41.8$ km (\cdots). At the subsequent cross-sections the traffic situation recovers ($- - -$: $r = r_0 + 1$ km; $- \cdot -$: $r = r_0 + 2.2$ km; $-$: $r = r_0 + 4.2$ km). Nevertheless, the amplitudes of the small velocity fluctuations at r_0 become larger and larger, leading to so-called stop-and-go waves, i.e. to alternating periods of decelerating and accelerating traffic.

In section 2 it will be shown that most proposed macroscopic traffic models can be viewed as special cases of the *continuity equation*

$$\frac{\partial \rho}{\partial t} + \frac{\partial \mathcal{Q}}{\partial r} = 0 \quad \text{with} \quad \mathcal{Q} = \rho V \quad (1)$$

for the spatial *density* $\rho(r, t)$ per lane and and a *velocity equation* of the form

$$\frac{\partial V}{\partial t} + V \frac{\partial V}{\partial r} = -\frac{1}{\rho} \frac{\partial \mathcal{P}}{\partial r} + \frac{1}{\tau} [V_e(\rho) - V]. \quad (2)$$

Here, $V \partial V / \partial r$ is the so-called *convection term* (*transport term*) which describes velocity changes arising from the motion with mean velocity V . The term containing the *traffic pressure* \mathcal{P} is the *anticipation term* and takes into account that driver-vehicle units react to the traffic situation in front of them. The *relaxation term* $(V_e - V)/\tau$ reflects the adaptation of the *mean velocity* $V(r, t)$ to the density-dependent *equilibrium velocity* $V_e(\rho)$ (cf. Fig. 3) with a *relaxation time* τ .

Apart from the relaxation term, the continuity equation and the velocity equation have the form of the fluid-dynamic equations for compressible gases. The additional relaxation term reflects that the mean velocity of vehicles decreases at bottlenecks, in contrast to ordinary fluids which flow faster. Later on, it will turn out that the relaxation term is responsible for the emergence of stop-and-go traffic.

It should be remarked that all macroscopic traffic models of the above type base on phenomenological reasoning in a number of points. Therefore, they imply at least one of the following inconsistencies [12, 7, 2, 6], depending on the respective model (details later):

- The variation of individual vehicle velocities is neglected. Some models take it into account by the dependence $\mathcal{P} = \rho \Theta$ of the traffic pressure \mathcal{P} on the velocity variance Θ .
- The velocity variance does not decrease with growing density.
- The variance does not vanish when the mean velocity vanishes. Therefore, large pressure gradients, which can cause the development of negative velocities, are possible (cf. Eq. (2)).
- Vehicles are implicitly treated as point-like objects.
- For a certain density range, the traffic pressure decreases with growing density. This is connected with an acceleration of vehicles into regions with larger density (cf. Eq. (2)), so that drivers would race into existing traffic jams.

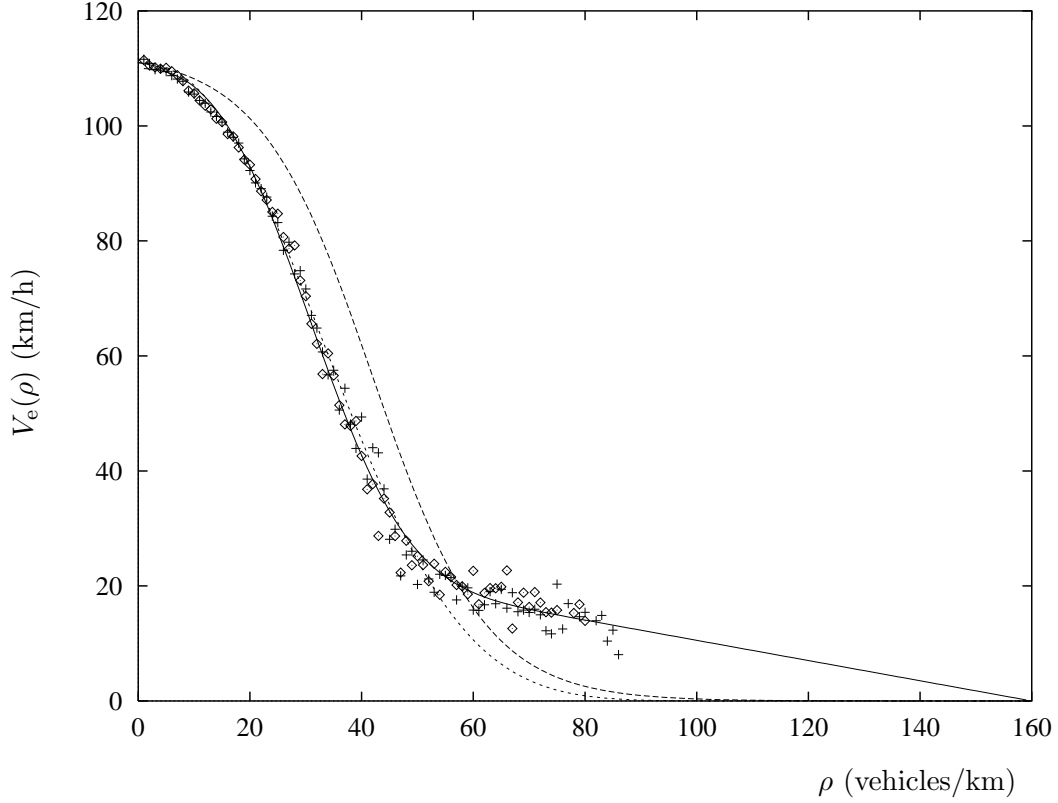


Figure 3: Illustration of different suggestions for the equilibrium velocity-density relation $V_e(\rho)$ (—: Helbing [9]; - -: Kerner and Konhäuser [5]; - . -: Kühne [10] and Cremer [11]), compared with empirical traffic data of the Dutch highway A9 from Haarlem to Amsterdam, where a speed limit of $V_0 = 120$ km/h applies (\diamond : October 14, 1994; $+$: November 2, 1994). The empirical data are mean values of all one minute averages which fall into the range $[\rho - 0.5 \text{ veh/km}, \rho + 0.5 \text{ veh/km}]$. $V_e(0) < V_0$ is because of the law that speedometers must show the actual speed or more, but never less.

- In the course of time, the density $\rho(r, t)$ can, on certain conditions, exceed the bumper-to-bumper density $\rho_{\text{bb}} = 1/l_0$, where l_0 denotes the average vehicle length.
- The region of unstable traffic flow, which is related with stop-and-go traffic, is not correctly described. In reality, traffic is only stable at very small densities (free flow) and extreme densities (slow-moving traffic).
- Emerging density waves develop a shock-like (i.e. almost discontinuous) structure.
- The viscosity terms which are implicitly (by the integration method) or explicitly introduced for a numerical solution of the macroscopic traffic equations have no theoretical foundation.

In this paper we will show, how to derive a consistent model from a suitable gas-kinetic (Boltzmann-like) model. For this purpose, we will extend Pavari-Fontana's Boltzmann-like model (cf. Sec. 3) by diffusion effects due to imperfect driving (cf. Sec. 4). Moreover, we have to take into account the space requirement by vehicles. This will be done analogously to the theory of dense gases and granular flows [13] (cf. Sec. 5). It will turn out that the structure of the resulting fluid-dynamic traffic equations changes considerably compared to Eqs. (1) and (2), as well as compared to the equations for dense gases or granular materials (cf. Sec. 5.1). Reasons for this are the loss of momentum conservation, the anisotropy of vehicular interactions, and the velocity-dependence of vehicular space requirements. Consequently, a direct transfer of relations for ordinary gases or fluids as proposed by previous traffic models is not possible.

2 Historical evolution of macroscopic traffic models

From equations (1) and (2) we obtain the traffic models suggested by other researchers, if \mathcal{P} , V_e , and τ are specified in a suitable way:

- In the limit $\tau \rightarrow 0$ we have

$$V(r, t) \approx V_e(\rho(r, t)). \quad (3)$$

The resulting model

$$\frac{\partial \rho}{\partial t} + \left(V_e + \rho \frac{\partial V_e}{\partial \rho} \right) \frac{\partial \rho}{\partial r} = 0 \quad (4)$$

was independently proposed by Lighthill and Whitham [14] and Richards [15]. It describes the formation of *kinematic waves* which propagate with velocity

$$c(\rho) = \rho \frac{\partial V_e}{\partial \rho} \quad (5)$$

relative to V_e . Nevertheless, the model cannot describe the emergence of stop-and-go traffic, since wave amplitudes are not amplified. The wave profile only becomes steeper and steeper in the course of time, so that it builds up a shock-like structure (i.e. it becomes discontinuous). Consequently, a simulation of Eq. (4) is very problematic. Numerically treatable variants of the above model were developed by Daganzo [16].

- Payne [17] suggested the model

$$\frac{\partial V}{\partial t} + V \frac{\partial V}{\partial r} \equiv \frac{dV}{dt} = -\frac{1}{\tau} \left(V - V_e - \frac{\partial \rho / \partial r}{2\rho} \frac{\partial V_e}{\partial \rho} \right) = -\frac{\nu}{\rho \tau} \frac{\partial \rho}{\partial r} + \frac{1}{\tau} (V_e - V) \quad (6)$$

with $\nu = \frac{1}{2} |\partial V_e / \partial \rho|$, corresponding to the traffic pressure

$$\mathcal{P} = -V_e / (2\tau). \quad (7)$$

He derived his model from a microscopic follow-the-leader model [18] by means of a Taylor expansion [17]. This model was also used by Papageorgiou [19]. Cremer [20] slightly modified the anticipation term by a factor $\rho / (\rho + \varkappa)$. Finally, Smulders [21] introduced additional fluctuation terms in the continuity and velocity equation. However, the resulting equations still predict the development of shock-like density changes, if no “*numerical viscosity*” is introduced.

- In the limit $\tau \rightarrow 0$, Payne’s model implies

$$V(r, t) = V_e(\rho(r, t)) - \frac{\tau}{\rho} \frac{\partial \mathcal{P}}{\partial \rho} \frac{\partial \rho(r, t)}{\partial r}. \quad (8)$$

This results in an additional diffusion term to the Lighthill-Whitham-Richards model,

$$\frac{\partial \rho}{\partial t} + \left(V_e + \rho \frac{\partial V_e}{\partial \rho} \right) \frac{\partial \rho}{\partial r} = \mathcal{D} \frac{\partial^2 \rho}{\partial r^2}, \quad (9)$$

which solves the shock-formation problem. The diffusion function is

$$\mathcal{D} = \tau \frac{\partial \mathcal{P}}{\partial \rho} = \frac{1}{2} \left| \frac{\partial V_e}{\partial \rho} \right|. \quad (10)$$

- A discrete cell model which is very suitable for real-time simulations of large traffic networks was proposed by Hilliges and Weidlich [3]. This consists of the discrete continuity equation

$$\frac{\partial \rho(i, t)}{\partial t} + \frac{1}{\Delta r} [\mathcal{Q}(i, t) - \mathcal{Q}(i - 1, t)] = 0. \quad (11)$$

Due to the anticipatory driver behavior the flow is modelled by

$$\mathcal{Q}(i, t) := \rho(i, t) V_e(\rho(i + 1, t)), \quad (12)$$

which assumes that drivers adapt to the velocity in the next cell. Therefore, the cell length $\Delta r \approx 100$ m must be chosen in agreement with the driver behavior. By Taylor approximation of the Hilliges-Weidlich model, we again obtain equation (9), but this time the diffusion function is given by

$$\mathcal{D} = \frac{\Delta r}{2} \left(V_e + \rho \left| \frac{\partial V_e}{\partial \rho} \right| \right). \quad (13)$$

In the special case

$$V_e(\rho) = V_0 \left(1 - \frac{\rho}{\rho_{\max}} \right), \quad (14)$$

equation (9) can be transformed to the analytically solvable Burgers equations [22]

$$\frac{\partial C}{\partial t} + C(r, t) \frac{\partial C}{\partial r} = \mathcal{D} \frac{\partial^2 C}{\partial r^2} \quad (15)$$

with

$$C(r, t) = V_0 \left(1 - \frac{2\rho(r, t)}{\rho_{\max}} \right). \quad (16)$$

Since the stationary solutions of Eq. (9) are stable with respect to fluctuations, the above model cannot describe the formation of stop-and-go waves. Therefore, an extension by a dynamic velocity equation of the form (2) with $\mathcal{P} = 0$ was proposed [3].

- An alternative approach to the model of Payne was suggested by Phillips [23], who derived his model from a Boltzmann-like traffic equation. For the traffic pressure he obtained the gas-kinetic relation

$$\mathcal{P} = \rho \Theta, \quad (17)$$

where he assumed

$$\Theta(\rho) = \Theta_0 \left(1 - \frac{\rho}{\rho_{\max}} \right), \quad (18)$$

since the *velocity variance* Θ should vanish at the *maximum traffic density* ρ_{\max} . However, according to this formula the density-gradient $\partial\mathcal{P}/\partial\rho$ of the traffic pressure will be negative in a certain density range (cf. Fig. 10).

- Kühne [4] as well as Kerner, and Konhäuser [5] avoided this problem by assuming $\Theta(\rho) = \Theta_0$. However, Θ cannot be interpreted as velocity variance, then, so that their equations are not compatible with gas-kinetic traffic models. Moreover, in order to smooth out developing shock structures, Kühne introduced an additional *viscosity term* $\tilde{\nu}\partial^2V/\partial r^2$ [4]. In analogy to the Navier-Stokes equations for ordinary fluids, Kerner and Konhäuser assumed $\tilde{\nu}(\rho) = \eta_0/\rho$, so that their model corresponds to the effective traffic pressure

$$\mathcal{P} = \mathcal{P}_e - \eta_0 \frac{\partial V}{\partial r} \quad \text{with} \quad \mathcal{P}_e = \rho\Theta_0. \quad (19)$$

Simulations of their model show the formation of density clusters and stop-and-go waves at moderate densities [5]. The instability region can be determined by a *linear stability analysis* about the stationary and spatially homogeneous solution $\rho(r, t) = \rho_e$ and $V(r, t) = V_e(\rho_e)$. Inserting the small overall perturbation

$$\begin{aligned} \delta\rho(r, t) &:= \rho(r, t) - \rho_e = \int dk \hat{\rho}(k) \exp[ikr + (\lambda - i\omega)t], \\ \delta V(r, t) &:= V(r, t) - V_e(\rho_e) = \int dk \hat{V}(k) \exp[ikr + (\lambda - i\omega)t] \end{aligned} \quad (20)$$

into Eqs. (1) and (2), applying a Taylor expansion, neglecting non-linear contributions, and applying the orthogonality relations for the complex exponential functions yields the following linear eigenvalue problem:

$$\begin{pmatrix} -\tilde{\lambda} & -ik\rho_e \\ -\frac{ik}{\rho_e} \frac{\partial\mathcal{P}_e}{\partial\rho} + \frac{1}{\tau} \frac{\partial V_e}{\partial\rho} & -\tilde{\lambda} - \frac{\eta_0 k^2}{\rho_e} - \frac{1}{\tau} \end{pmatrix} \begin{pmatrix} \hat{\rho}(k) \\ \hat{V}(k) \end{pmatrix} \stackrel{!}{=} \begin{pmatrix} 0 \\ 0 \end{pmatrix}. \quad (21)$$

Here, we have introduced the abbreviation

$$\tilde{\lambda} := \lambda - i\tilde{\omega} \quad \text{with} \quad \tilde{\omega} := \omega - kV_e(\rho_e). \quad (22)$$

k is the *wave number*, λ the *growth parameter*, and ω the *oscillation frequency* of the perturbations. Eq. (21) is fulfilled for the solutions of the *characteristic polynomial*

$$\tilde{\lambda}^2 + \tilde{\lambda} \left(\frac{\eta_0 k^2}{\rho_e} + \frac{1}{\tau} \right) + ik\rho_e \left(-\frac{ik}{\rho_e} \frac{\partial \mathcal{P}_e}{\partial \rho} + \frac{1}{\tau} \frac{\partial V_e}{\partial \rho} \right) = 0. \quad (23)$$

This leads to

$$\begin{aligned} \tilde{\lambda} &= -\frac{1}{2T} \pm \sqrt{\frac{1}{4T^2} - (C_r + iC_i)} = -\frac{1}{2T} \pm \sqrt{\Re \pm i|\Im|} \\ &= -\frac{1}{2T} \pm \left[\sqrt{\frac{1}{2} \left(\sqrt{\Re^2 + \Im^2} + \Re \right)} \pm i \sqrt{\frac{1}{2} \left(\sqrt{\Re^2 + \Im^2} - \Re \right)} \right], \end{aligned} \quad (24)$$

where we have defined

$$\frac{1}{T} := \frac{\eta_0 k^2}{\rho_e} + \frac{1}{\tau}, \quad C_r := k^2 \frac{\partial \mathcal{P}_e}{\partial \rho}, \quad C_i := \frac{k\rho_e}{\tau} \frac{\partial V_e}{\partial \rho}, \quad (25)$$

and

$$\Re := \frac{1}{4T^2} - C_r = \frac{1}{4T^2} - k^2 \frac{\partial \mathcal{P}_e}{\partial \rho}, \quad \pm|\Im| := -C_i = \frac{k\rho_e}{\tau} \left| \frac{\partial V_e}{\partial \rho} \right|. \quad (26)$$

A transition from stability to instability occurs on the condition

$$\lambda = -\frac{1}{2T} \pm \sqrt{\frac{1}{2} \left(\sqrt{\Re^2 + \Im^2} + \Re \right)} \stackrel{!}{=} 0 \quad (27)$$

which implies

$$C_i \stackrel{!}{=} \pm \frac{1}{T} \sqrt{C_r}. \quad (28)$$

Therefore, the equilibrium solution of the Kühne-Kerner-Konhäuser model is unstable on the condition

$$\rho_e \left| \frac{\partial V_e}{\partial \rho} \right| > \sqrt{\frac{\partial \mathcal{P}_e}{\partial \rho}} \left(1 + \frac{\tau \eta_0 k^2}{\rho_e} \right). \quad (29)$$

This condition is fulfilled at moderate densities, where the equilibrium velocity V_e rapidly decreases with growing density (cf. Figs. 3 and 4a). According to the continuity equation (1), this decrease of velocity causes a further increase of density which finally leads to the formation of density clusters. Short wave lengths (i.e. large wave numbers) are stable because of the smoothing effect of viscosity η_0 .

The propagation speed of small perturbations relative to $V_e(\rho_e)$ is given by the relative *group velocity*

$$c(\rho_e, k) := \frac{\partial}{\partial k} \tilde{\omega}(\rho_e, k) = \pm \frac{\partial}{\partial k} \sqrt{\frac{1}{2} \left(\sqrt{\Re^2 + \Im^2} - \Re \right)} \quad (30)$$

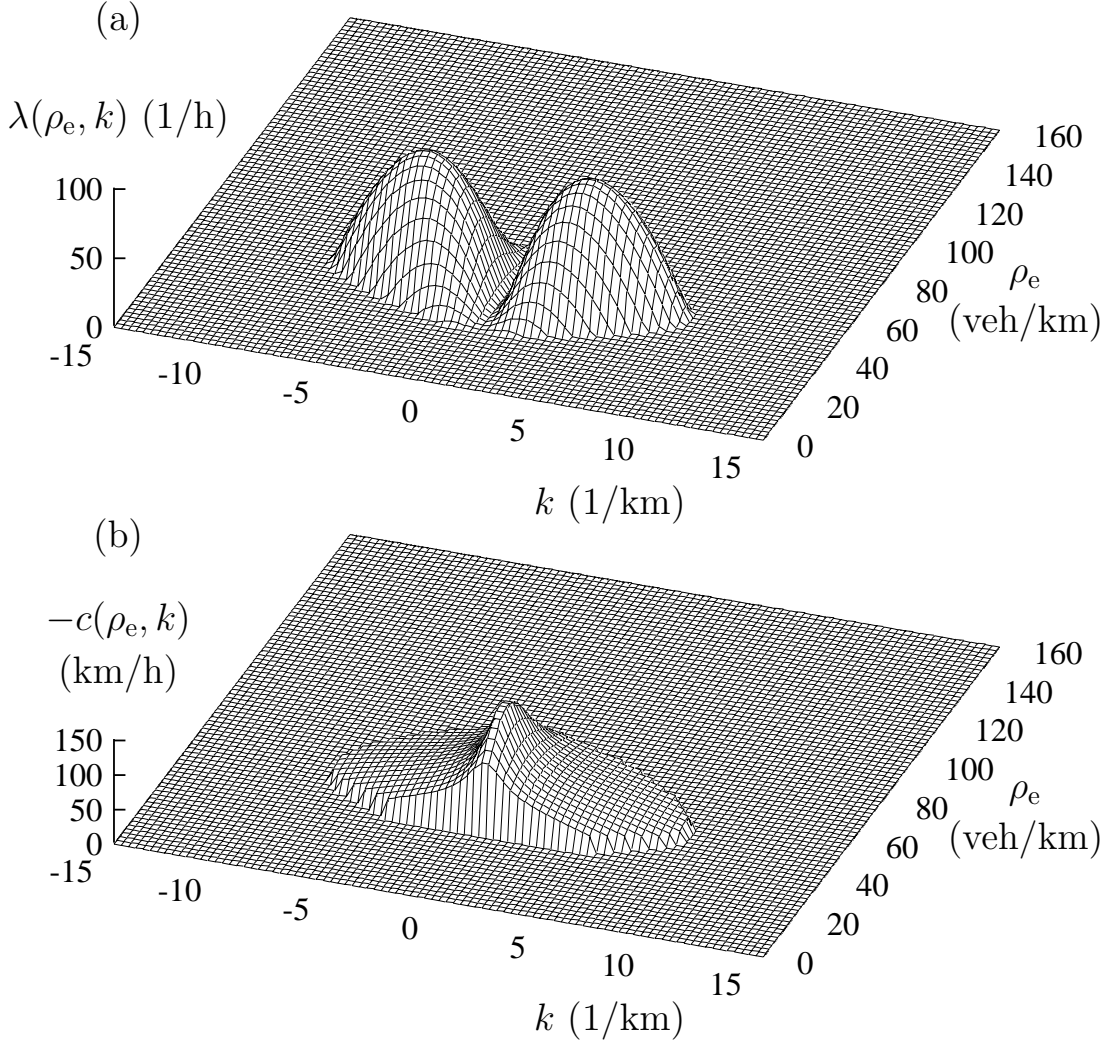


Figure 4: (a) Illustration of the largest growth parameter λ for the instability region (i.e. where $\lambda(\rho_e, k) \geq 0$). According to the Kühne-Kerner-Konhäuser model (with $\tau = 11$ s, $\eta_0 = 436$ km/h, $\sqrt{\Theta_0} = 54$ km/h, and the equilibrium velocity $V_e(\rho)$ depicted in Fig. 3) traffic flow is unstable at moderate densities and small absolute wavelengths $|k|$. At $k = 0$ we have marginal stability (i.e. $\lambda(\rho_e, 0) = 0$) due to the conservation of the number of vehicles. Instabilities at large absolute wave numbers $|k|$ (i.e. small wave lengths) are suppressed by the smoothing effect of viscosity. Although the model describes the instability region qualitatively right, practical experience indicates that stop-and-go traffic also develops at much higher densities.

(b) The representation of the negative group velocity of the unstable mode relative to V_e shows that emerging stop-and-go waves move in backward direction, as expected. However, the relative propagation speeds seem to be somewhat too large.

(cf. Fig. 4b). At the transition from stability to instability we find

$$c(\rho_e, k) = \pm \frac{1}{k} \sqrt{C_r} = \pm \sqrt{\frac{\partial \mathcal{P}_e}{\partial \rho}}. \quad (31)$$

This formula is analogous to the one for the velocity of sound in ordinary compressible fluids. However, for traffic flows, the plus sign corresponds to the stable mode and the minus sign to the unstable mode, so that the forming stop-and-go waves move in backward direction. This is in agreement with empirical findings and solves a problem raised by Daganzo [12].

- Helbing [2, 6] introduced a further dynamic equation for the variance,

$$\frac{\partial \Theta}{\partial t} + V \frac{\partial \Theta}{\partial r} = -\frac{2\mathcal{P}}{\rho} \frac{\partial V}{\partial r} - \frac{1}{\rho} \frac{\partial \mathcal{J}}{\partial r} + \frac{2}{\tau} (\Theta_e - \Theta), \quad (32)$$

which bases on a gas-kinetic traffic model. This equation is analogous to the equation of *heat conduction*. However, it contains an additional relaxation term $2(\Theta_e - \Theta)/\tau$. Moreover, despite their theoretical relationship, the variance Θ is better not denoted as temperature, and \mathcal{J} is not a heat flow but the *flux density of velocity variance*.

Another modification suggested by Helbing intended to take into account the finite space requirements $s(V)$ by vehicles. In analogy to the pressure relation of van der Waals for a gas of hard spheres (cf. Eq. (93)), he proposed the relation

$$\mathcal{P} = \frac{\rho \Theta}{1 - \rho s(V)}. \quad (33)$$

However, in Section 5.2 it will turn out that this relation cannot simply be transferred from the theory of ordinary gases to the theory of traffic flow: The dissipative and anisotropic interactions of vehicles as well as their velocity-dependent space requirements change the structure of the fluid-dynamic traffic equations considerably.

3 Paveri-Fontana's gas-kinetic traffic model

Prigogine and coworkers [24] were the first who proposed the derivation of macroscopic traffic equations from a gas-kinetic level of description. However, Paveri-Fontana [25] noticed some strange properties of their approach and suggested a modified model which will now be discussed. This model describes the temporal evolution of the *phase-space*

density $\hat{\rho}(r, v, v_0, t)$ of vehicles with *desired velocity* v_0 and (*actual*) *velocity* v at place r and time t , which is governed by the *continuity equation*

$$\frac{\partial \hat{\rho}}{\partial t} + \frac{\partial}{\partial r}(\hat{\rho}v) + \frac{\partial}{\partial v} \left(\hat{\rho} \frac{dv}{dt} \right) + \frac{\partial}{\partial v_0} \left(\hat{\rho} \frac{dv_0}{dt} \right) = \left(\frac{\partial \hat{\rho}}{\partial t} \right)_{\text{dis}}. \quad (34)$$

The *acceleration law* was specified by

$$\frac{dv}{dt} = \frac{v_0 - v}{\tau}, \quad (35)$$

delineating an exponential adaptation of the actual velocity v to the individual desired velocity v_0 with a density-dependent relaxation time $\tau(\rho)$. Since the individual desired velocity v_0 is usually assumed to be constant, we have

$$\frac{dv_0}{dt} = 0. \quad (36)$$

According to Eq. (34), the substantial time derivative of the phase-space density is given by temporal changes $(\partial \hat{\rho} / \partial t)_{\text{dis}}$ due to *discontinuously* modelled velocity changes. Usually, *interaction processes* are delineated by this term, since they happen much faster than the acceleration processes [26]. Pavari-Fontana proposed to use the Boltzmann-like equation

$$\begin{aligned} \left(\frac{\partial \hat{\rho}}{\partial t} \right)_{\text{dis}} &= (1-p) \int_{w>v} dw \int dw_0 |w-v| \hat{\rho}(r, v, w_0, t) \hat{\rho}(r, w, v_0, t) \\ &- (1-p) \int_{w<v} dw \int dw_0 |v-w| \hat{\rho}(r, w, w_0, t) \hat{\rho}(r, v, v_0, t), \end{aligned} \quad (37)$$

assuming that a slower vehicle can be immediately overtaken with probability $p(\rho)$, and that the faster vehicle exactly decelerates to the velocity of the slower one, if this is not possible. Whereas the first term delineates an increase of $\hat{\rho}(r, v, v_0, t)$ due to vehicles with velocity $w > v$ that must decelerate to velocity v , the second term describes a decrease of $\hat{\rho}(r, v, v_0, t)$ due to vehicles with velocity v which must decelerate to a velocity $w < v$. According to (37), the interaction frequency of vehicles is proportional to their relative velocity $|v-w|$ and to the phase-space densities $\hat{\rho}$ of the interacting vehicles. Their desired velocities v_0 and w_0 are not changed by interactions.

The gas-kinetic equation allows a derivation of macroscopic traffic equations for the spatial vehicle *density*

$$\rho(r, t) := \int dv \int dv_0 \hat{\rho}(r, v, v_0, t) \quad (38)$$

and the *velocity moments*

$$\langle v^k (v_0)^l \rangle := \int dv \int dv_0 v^k (v_0)^l \frac{\hat{\rho}(r, v, v_0, t)}{\rho(r, t)}, \quad (39)$$

in particular the *mean velocity*

$$V(r, t) := \langle v \rangle = \int dv v P(v; r, t) \quad (40)$$

and the velocity *variance*

$$\Theta(r, t) := \langle (v - V)^2 \rangle = \int dv (v - V)^2 P(v; r, t), \quad (41)$$

where we have introduced the *velocity distribution*

$$P(v; r, t) := \int dv_0 \frac{\hat{\rho}(r, v, v_0, t)}{\rho(r, t)}. \quad (42)$$

The macroscopic equations are obtained by multiplication of the gas-kinetic equation (34) with $\psi(v) := 1, v, v^2$ and subsequent integration over v and v_0 . Finally, one finds the fluid-dynamic traffic equations

$$\frac{\partial \rho}{\partial t} + V \frac{\partial \rho}{\partial r} = -\rho \frac{\partial V}{\partial r}, \quad (43)$$

$$\frac{\partial V}{\partial t} + V \frac{\partial V}{\partial r} = -\frac{1}{\rho} \frac{\partial \mathcal{P}}{\partial r} + \frac{1}{\tau} (V_e - V), \quad (44)$$

$$\frac{\partial \Theta}{\partial t} + V \frac{\partial \Theta}{\partial r} = -\frac{2\mathcal{P}}{\rho} \frac{\partial V}{\partial r} - \frac{1}{\rho} \frac{\partial \mathcal{J}}{\partial r} + \frac{2}{\tau} (\Theta_e - \Theta), \quad (45)$$

which was shown in Refs. [6, 25]. We recognize that the density equation (43) and the velocity equation (44) have again the form of Eqs. (1) and (2). However, we have additionally found theoretical relations for the *traffic pressure*

$$\mathcal{P} := \rho \langle (v - V)^2 \rangle = \rho \Theta \quad (46)$$

and the *equilibrium velocity*

$$V_e := V_0 - \tau(\rho)[1 - p(\rho)]\rho\Theta. \quad (47)$$

Moreover, we have obtained the *variance equation* (45) with the *flux density of velocity variance*

$$\mathcal{J} := \rho \langle (v - V)^3 \rangle, \quad (48)$$

the *equilibrium variance*

$$\Theta_e := \mathcal{C} - \frac{1}{2}\tau(\rho)[1 - p(\rho)]\rho \langle (v - V)^3 \rangle, \quad (49)$$

and the *covariance*

$$\mathcal{C} := \langle (v - V)(v_0 - V_0) \rangle. \quad (50)$$

For the evaluation of $\mathcal{J}(r, t)$ we need a mathematical expression for the *velocity distribution* $P(v; r, t)$. This can be approximately obtained by Grad's method of moments [27], which uses the expansion

$$P(v; r, t) \approx \sum_{n=0}^N a_n(r, t) \frac{\partial^n}{\partial v^n} \frac{1}{\sqrt{2\pi\Theta}} \exp \left[-\frac{(v - V)^2}{2\Theta} \right]. \quad (51)$$

The functions $a_n(r, t)$ can be expressed by the velocity moments $\langle v^k \rangle$ ($0 \leq k \leq N$) which are governed by the macroscopic equations. In gas theory the macroscopic equations are closed after the variance equation ($N = 2$), since higher velocity moments are varying on much faster time scales, so that their adiabatic elimination is justified. For vehicular traffic as for granular materials, a separation of time scales is not this simple. Therefore, one usually restricts to the number N of macroscopic equations, which allow to delineate the instabilities under consideration. Sela and Goldhirsch [29] have shown that this method yields reliable and “universal” results in the sense that the inclusion of additional macroscopic equations gives no fundamental but only minor corrections.

From our discussion in Sec. 2 we know that the continuity and velocity equation are sufficient for a description of emerging stop-and-go traffic. Therefore, we choose $N = 1$, so that we must express $\Theta(r, t)$ in dependence of $\rho(r, t)$ and $V(r, t)$:

$$\Theta(r, t) := \Theta_e(\rho(r, t), V(r, t)). \quad (52)$$

Because of the conditions $\langle 1 \rangle \stackrel{!}{=} 1$ and $\langle v \rangle \stackrel{!}{=} V(r, t)$, we find $a_0(r, t) = 1$ and $a_1(r, t) = 0$, so that we get the Gaussian distribution

$$P(v; r, t) \approx \frac{1}{\sqrt{2\pi\Theta_e}} \exp \left[-\frac{(v - V)^2}{2\Theta_e} \right]. \quad (53)$$

This leads to [6]

$$\mathcal{J} = 0 \quad \text{and} \quad \Theta_e = \mathcal{C}_e, \quad (54)$$

where \mathcal{C}_e is the *equilibrium covariance* (cf. Fig. 6). In Ref. [6] it has been shown that \mathcal{C}_e is given by the implicit equation

$$\mathcal{C}_e = \langle (v_0 - V_0)^2 \rangle - 2\tau(\rho)[1 - p(\rho)]\rho\mathcal{C}_e\sqrt{\frac{\Theta_e}{\pi}}. \quad (55)$$

Therefore, Θ_e is only a function of ρ and not of V (cf. Fig. 7): Eqs. (54) and (55) together with (47) imply the relation

$$\sqrt{\Theta_e(\rho)} = -\frac{V_0 - V_e(\rho)}{\sqrt{\pi}} + \sqrt{\frac{[V_0 - V_e(\rho)]^2}{\pi} + \langle (v_0 - V_0)^2 \rangle}. \quad (56)$$

In homogeneous traffic situations, the *variance of desired velocities* $\Theta_0 := \langle (v_0 - V_0)^2 \rangle$ should be a constant and, in particular, independent of density. Therefore, relation (56) predicts that the variance is still finite when the equilibrium velocity V_e vanishes. This is, of course, a paradoxical result.

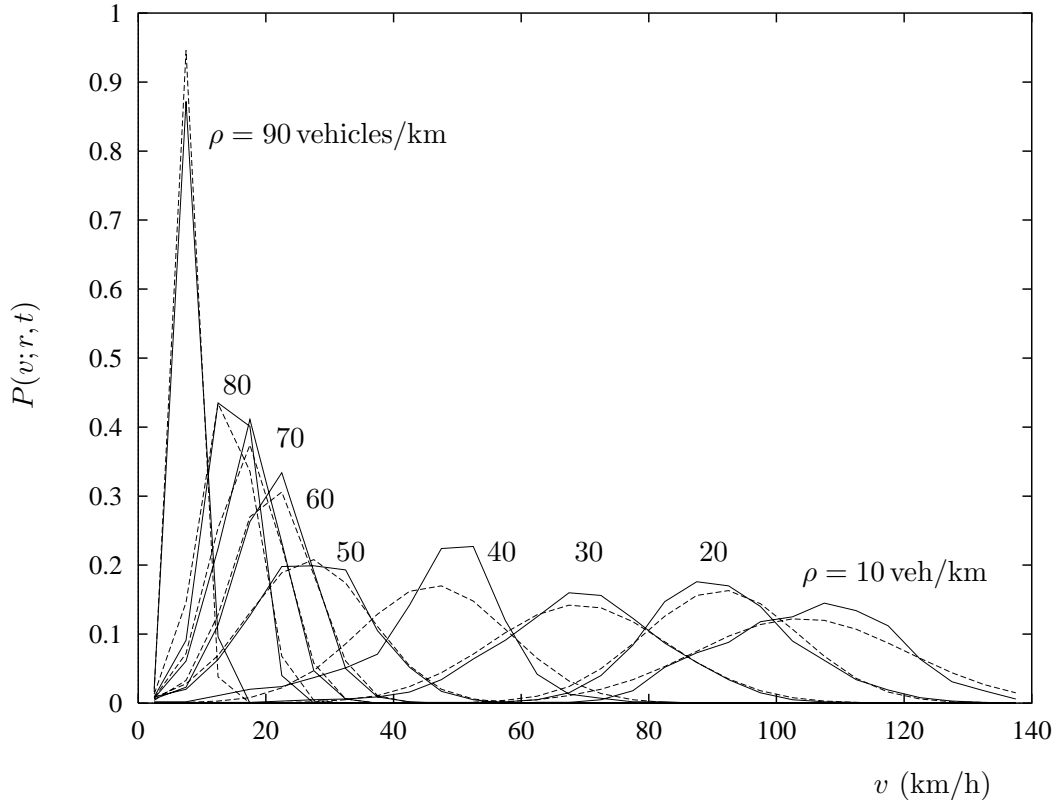


Figure 5: Comparison of empirical velocity distributions at different densities (—) with frequency polygons of grouped Gaussian velocity distributions with the same mean value and variance (---). The class interval lengths are 5 km/h. A significant deviation of the empirical relations from the respective discrete Gaussian approximations is only found at density $\rho = 40$ vehicles/km, where the two minute averages of the single vehicle data may have been too long due to rapid stop-and-go waves (cf. the mysterious “knee” at $\rho \approx 40$ veh/km in Fig. 7). The velocity distributions keep their unimodal form even at high densities. (Data: Dutch highway A9 with constant speed limit 120 km/h.)

Another problem was recognized by Shvetsov [28]: According to Pavari-Fontana’s equation, vehicles are not decelerated to velocities less than the minimum desired velocity of all drivers. Therefore, it cannot describe the development of so-called *phantom traffic jams*, where all drivers want to drive fast, but produce a slowly moving traffic jam.

As a consequence, we must modify Pavari-Fontana’s equation somewhat. This is done in

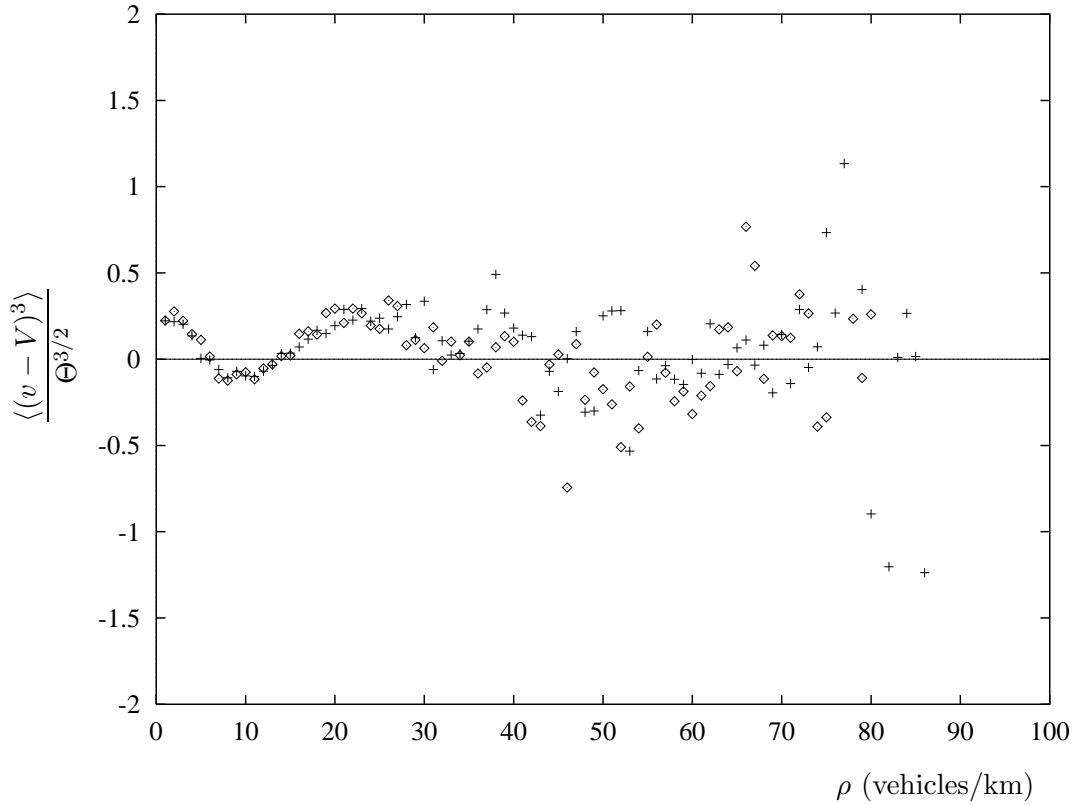


Figure 6: Empirical skewness of the velocity distribution on the basis of mean values of one minute averages (\diamond : October 14, 1994; $+$: November 2, 1994). The absolute value of the skewness is rather small and mostly lies between 0 and 0.5. (The variation of the data at higher densities results from the small amount of one minute data that could be averaged.)

the next two sections.

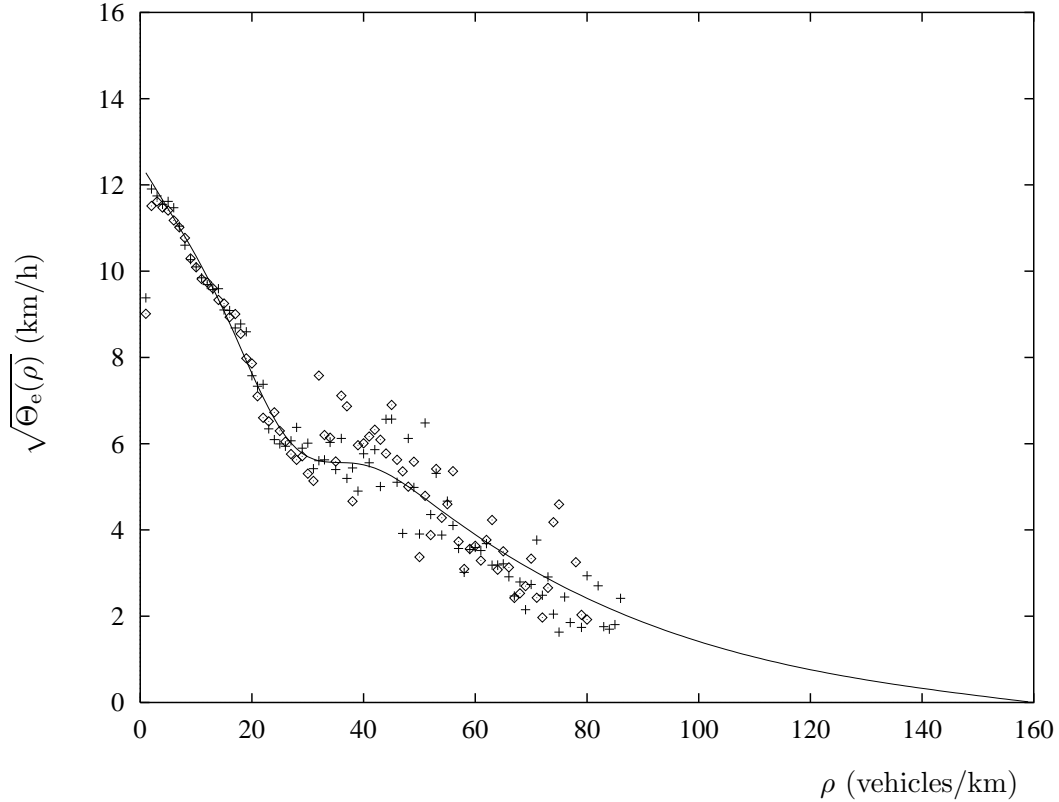


Figure 7: Illustration of the empirical equilibrium variance-density relation $\Theta_e(\rho)$, evaluated like in Fig. 3 (\diamond : October 14, 1994; $+$: November 2, 1994; $—$: fit function).

4 Imperfect driving

Up to now, we have assumed perfectly driving vehicles that are able to keep a constant speed and to exactly adapt to the velocity of a slower vehicle in front. Therefore, we will replace Paveri-Fontana's interaction term by the more general formula

$$\left(\frac{\partial \hat{\rho}}{\partial t}\right)_{\text{dis}} := \left(\frac{\partial \hat{\rho}}{\partial t}\right)_{\text{diff}} + \left(\frac{\partial \hat{\rho}}{\partial t}\right)_{\text{int}}, \quad (57)$$

where

$$\left(\frac{\partial \hat{\rho}}{\partial t}\right)_{\text{diff}} := \frac{1}{2} \frac{\partial^2}{\partial v^2} (\mathcal{D} \hat{\rho}) \quad (58)$$

describes *velocity fluctuations* due to imperfect speed control. The diffusion function \mathcal{D} must be chosen in such a way that the velocity-diffusion term $(\partial \hat{\rho} / \partial t)_{\text{diff}}$ cannot produce

negative velocities. In the following, we will assume

$$D(v) = \frac{2\alpha v^2}{\tau} \quad (59)$$

in order to obtain a dimensionless relation $\alpha(\rho)$. According to Eq. (59), velocity fluctuations are related to the time scale τ of velocity adaptation. Moreover, comparing (59) with the formula $\langle |\Delta x|^2 \rangle = \mathcal{D}\Delta t$ for spatial diffusion with diffusion constant \mathcal{D} , the absolute velocity displacement $|\Delta v|$ is approximately *proportional* to v during small time intervals Δt , which sounds plausible.

Now, we will generalize the interaction term. By

$$\begin{aligned} \left(\frac{\partial \hat{\rho}}{\partial t} \right)_{\text{int}} &= \int dw \int_{v' > w} dv' \int_{w' \geq v} dw' \int dw_0 |w - v'| \sigma(w', v|w, v') \hat{\rho}(r, w, w_0, t) \hat{\rho}(r, v', v_0, t) \\ &- \int_{w < v} dw \int dv' \int_{w' \geq v'} dw' \int dw_0 |v - w| \sigma(w', v'|w, v) \hat{\rho}(r, w, w_0, t) \hat{\rho}(r, v, v_0, t) \end{aligned} \quad (60)$$

we can take into account vehicles that do not exactly adapt to the velocity of a slower car in front. $\sigma(w', v'|w, v)$ denotes the *differential cross section* and describes the probability with which two vehicles have velocities v' and w' after their interaction, if they had velocities v and w before. In the following, we will choose

$$\sigma(w', v'|w, v) := \frac{1-p}{\beta w} \exp\left(-\frac{w-v'}{\beta w}\right) \delta(w' - w) \quad (61)$$

where $\delta(\cdot)$ denotes Dirac's delta function. According to this formula, the velocity w of the slower vehicle is not influenced by the velocity of a faster vehicle with velocity v behind it (i.e. $w' = w$). The exponential function reflects that the faster vehicle slows down to a velocity $v' \leq w$. Although the velocity $v' = w$ is most likely, smaller velocities $v' < w$ also occur with a certain probability due to an imperfect adaptation of velocity. For the degree β of imperfection we have $0 \leq \beta \ll 1$. In the limit $\beta = 0$, formula (61) becomes $\sigma(w', v'|w, v) = (1-p)\delta(v' - w)\delta(w' - w)$, so that we get back Pavri-Fontana's interaction term (37).

In order to obtain the macroscopic traffic equations corresponding to the generalized

gas-kinetic equation, we have to evaluate the interaction terms

$$\begin{aligned}
\mathcal{I}(\psi) &:= \int dv \int dv_0 \psi(v) \left(\frac{\partial \hat{\rho}}{\partial t} \right)_{\text{int}} \\
&= \rho^2(r, t) \int dv \int_{v' > w} dw \int_{w' \geq v} dv' \int dw' \psi(v) |w - v'| \sigma(w', v | w, v') P(w; r, t) P(v'; r, t) \\
&\quad - \rho^2(r, t) \int dv \int_{w < v} dw \int_{w' \geq v'} dv' \int dw' \psi(v) |v - w| \sigma(w', v' | w, v) P(w; r, t) P(v; r, t) \\
&= \rho^2(r, t) \int_{w < v} dv \int dw \int_{w' \geq v'} dv' \int dw' |v - w| \sigma(w', v' | w, v) \\
&\quad \times [\psi(v') - \psi(v)] P(w; r, t) P(v; r, t), \tag{62}
\end{aligned}$$

where we have interchanged variables to obtain the final result. With (53) and (61) we find $\mathcal{I}(1) = 0$ and

$$\begin{aligned}
\mathcal{I}(v) &= -(1-p)\rho^2 \left[\Theta_e \left(1 - \frac{\beta}{2} \right) + \beta V \sqrt{\frac{\Theta_e}{\pi}} \right], \\
\mathcal{I}((v-V)^2) &\approx (1-p)\rho^2 \left(\beta V \Theta_e + 2\beta^2 V^2 \sqrt{\frac{\Theta_e}{\pi}} \right). \tag{63}
\end{aligned}$$

Since the diffusion term $(\partial \hat{\rho} / \partial t)_{\text{diff}}$ yields no contribution to the density and velocity equation, but the contribution $2\alpha(V^2 + \Theta_e)/\tau$ to the variance equation, we arrive at the corrected equilibrium relations

$$V_e(\rho, V) = V_0 - \tau(1-p)\rho \left[\Theta_e \left(1 - \frac{\beta}{2} \right) + \beta V \sqrt{\frac{\Theta_e}{\pi}} \right], \tag{64}$$

$$\Theta_e(\rho, V) = \mathcal{C}_e + \alpha(V^2 + \Theta_e) + \frac{\tau}{2}(1-p)\rho \left(\beta V \Theta_e + 2\beta^2 V^2 \sqrt{\frac{\Theta_e}{\pi}} \right). \tag{65}$$

Note that the equilibrium relations V_e and Θ_e not only depend on the density ρ , but also on the mean velocity V , now. The previous formulas result for $\alpha = \beta = 0$.

4.1 Determination of the parameters from empirical data

The calibration of the functions $\alpha(\rho)$, $\beta(\rho)$, $p(\rho)$, and $\tau(\rho)$ is a difficult problem, since we only have empirical relations for $V_e(\rho)$ and $\Theta_e(\rho)$ (cf. Figs. 3 and 7). Therefore, we set $\beta = 0$ in order to reduce the number of parameters. (Setting $\alpha = 0$ does not allow to describe the finite equilibrium variance at small densities if $\mathcal{C}_e = 0$, see below.) Since the

equilibrium covariance \mathcal{C}_e is not anymore given by relation (55), we calculate it via Eq. (65):

$$\mathcal{C}_e(\rho) = (1 - \alpha)\Theta_e(\rho, V_e(\rho)) - \alpha[V_e(\rho)]^2. \quad (66)$$

This expression is completely determined by $V_e(\rho)$ and $\Theta_e(\rho)$, if we define

$$\alpha := \lim_{\rho \rightarrow \rho_{\max}} \frac{\Theta_e(\rho, V_e(\rho))}{[V_e(\rho)]^2 + \Theta_e(\rho, V_e(\rho))}. \quad (67)$$

Consequently, the equilibrium variance

$$\Theta_e(\rho, V) = \frac{\mathcal{C}_e(\rho) + \alpha V^2}{1 - \alpha} \quad (68)$$

is given by the diffusion effect $\alpha V^2/(1 - \alpha)$ at high densities, whereas it is dominated by the covariance \mathcal{C}_e at low densities, which is very plausible. In the case of speed limits, however, we have $\mathcal{C}_e \approx 0$, since all vehicles have approximately the same desired velocity $v_0 \approx V_0$. In this situation we define

$$\alpha(\rho) := \frac{\Theta_e(\rho, V_e(\rho))}{[V_e(\rho)]^2 + \Theta_e(\rho, V_e(\rho))}. \quad (69)$$

The product $\tau(\rho)[1 - p(\rho)]$ can be easily obtained via Eq. (103), which is a generalization of Eq. (64):

$$\tau(\rho)[1 - p(\rho)] = \frac{V_0 - V_e(\rho)}{\rho \chi \Theta_e(\rho, V_e(\rho))}. \quad (70)$$

A determination of the factors $p(\rho)$ and $\tau(\rho)$ is only possible by means of additional assumptions. A detailed analysis shows that the relaxation time is given by the relation

$$\tau(\rho) = \frac{q(\rho)}{\tau_0}, \quad (71)$$

where $q(\rho)$ is the *proportion of freely moving vehicles* and $\tau_0 \approx 8$ s the relaxation time of vehicles which are not impeded during their acceleration [9]. In addition, a complicated relation of the form $p(\rho, q(\rho), V_e(\rho))$ can be derived (cf. Ref. [9]). The resulting density-dependent functions $q(\rho) = \tau_0/\tau(\rho)$ and $[1 - p(\rho)]$ are depicted in Figure 8. It is very important that, although $p(\rho)$ approaches the value 0 in the limit $\rho \rightarrow \rho_{\max}$, the relaxation time $\tau(\rho)$ remains finite, since the maximum density ρ_{\max} is somewhat less than the inverse of the *average vehicle length* l_0 .

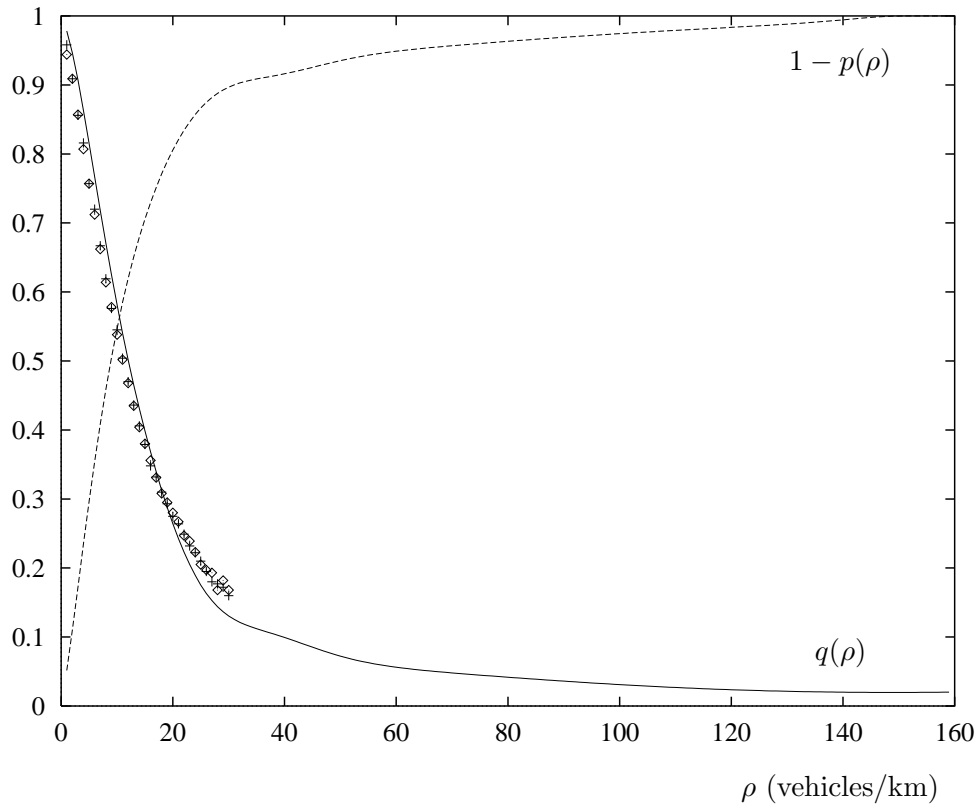


Figure 8: Illustration of different relations estimated from empirical traffic data: The density-dependent probability $(1 - p)$ that a fast car cannot immediately overtake a slower one (---) starts at zero and reaches the value one in the limit $\rho \rightarrow \rho_{\max}$. The proportion $q(\rho)$ of freely moving vehicles $q(\rho)$ is about one for very small densities and approaches a finite value with growing density (—). Symbols represent the proportion of vehicles that have a time headway greater than $2.5T$, where $T = 0.8$ s corresponds to the safe time headway (\diamond : October 14, 1994; $+$: November 2, 1994).

5 Dynamics at high densities

Up to now, vehicles have been implicitly treated as point-like objects. Therefore, the model must now be corrected for the finite space requirements of vehicles. This will lead to further modifications of the interaction term. In order to illustrate the applied method, we will first discuss the gas-kinetic and fluid-dynamic description of granular material like sand, powder, or pills [13, 29, 30].

5.1 Granular flow

Granular materials have found a broad interest due to their various instability phenomena like density waves, avalanches, cluster or heap formation, convection, or size segregation [31, 32]. In order to work out the similarities with traffic flow, we will focus on the description of density waves in sand falling through a narrow pipe [33]. Similar to the discussion by Riethmüller et al. [29] we assume a vertical tube of diameter s , in which spherical grains (or cylinders of height s) with radius $s/2$ are falling. Since grains do not have a desired velocity v_0 , we are confronted with the *phase-space density* $\tilde{\rho}(r, v, t)$ of grains with velocity v , this time. The corresponding gas-kinetic equation is

$$\frac{\partial \tilde{\rho}}{\partial t} + \frac{\partial}{\partial r}(\tilde{\rho}v) + \frac{\partial}{\partial v} \left(\tilde{\rho} \frac{dv}{dt} \right) = \frac{1}{2} \frac{\partial^2}{\partial v^2} (\mathcal{D} \tilde{\rho}) + \left(\frac{\partial \tilde{\rho}}{\partial t} \right)_{\text{int}}. \quad (72)$$

It exactly corresponds to the gas-kinetic traffic equation in the case of a speed limit V_0 , where the desired velocities of all drivers approximately agree ($v_0 \approx V_0$), so that v_0 is not a variable anymore, but a fixed parameter. Since velocity changes of grains result from *acceleration due to gravity* g as well as from sliding friction at the wall (and by displacement of air) with a *friction coefficient* γ , we have the acceleration law

$$\frac{dv}{dt} = g - \gamma v. \quad (73)$$

The diffusion term $\frac{1}{2} \mathcal{D} \partial^2 \tilde{\rho} / \partial v^2$ with *diffusion constant* $\mathcal{D} := 2\gamma\Theta_0$ describes variations of the grain velocities v due to fluctuating influences of the wall (and the displaced air) in accordance with the *fluctuation-dissipation theorem*.

Multiplying the gas-kinetic equation (72) with $\psi(v) := 1, v, \text{ or } v^2$, and integrating over v

gives the macroscopic equations

$$\frac{\partial \rho}{\partial t} + V \frac{\partial \rho}{\partial r} = -\rho \frac{\partial V}{\partial r}, \quad (74)$$

$$\frac{\partial V}{\partial t} + V \frac{\partial V}{\partial r} = -\frac{1}{\rho} \frac{\partial \mathcal{P}}{\partial r} + (g - \gamma V) + \frac{\mathcal{I}(v)}{\rho}, \quad (75)$$

$$\frac{\partial \Theta}{\partial t} + V \frac{\partial \Theta}{\partial r} = -\frac{2\mathcal{P}}{\rho} \frac{\partial V}{\partial r} - \frac{1}{\rho} \frac{\partial \mathcal{J}}{\partial r} + 2\gamma(\Theta_0 - \Theta) + \frac{\mathcal{I}((v - V)^2)}{\rho}, \quad (76)$$

where we have taken into account the conservation of the number of vehicles ($\mathcal{I}(1) = 0$). A comparison with the fluid-dynamic traffic equations shows that the equations agree with each other if we substitute $g \leftrightarrow V_0/\tau$, $\gamma \leftrightarrow 1/\tau$, $\Theta_0 \leftrightarrow \alpha(V^2 + \Theta)$, and specify the interaction term like in Eq. (37) with $v_0 \equiv V_0 \equiv w_0$. Although this specification was suggested by Riethmüller et al. [29], we will apply the theoretical relations for dense gases and granular materials [13], instead, in order to include effects due to high densities and momentum conservation. The interaction terms have then the form

$$\begin{aligned} \mathcal{I}(\psi) &= \int_{w < v} dv \int dw \int_{w' \geq v'} dv' \int dw' |v - w| \sigma(w', v' | w, v) [\psi(v') - \psi(v)] \tilde{\rho}_2(r + s, w; r, v; t) \\ &+ \int_{w > v} dv \int dw \int_{w' \leq v'} dv' \int dw' |v - w| \sigma(v', w' | v, w) [\psi(v') - \psi(v)] \tilde{\rho}_2(r, v; r - s, w; t). \end{aligned} \quad (77)$$

In contrast to the formula (62) for vehicular interactions, we have an additional contribution due to backward interactions of grains (last term). Moreover, we have taken into account that pushed grains are located at places $r + s$ or $r - s$. Finally, the *pair distribution* function $\tilde{\rho}_2$ describes velocity-correlations between interacting grains.

The expression (77) can be simplified by interchanging variables:

$$\begin{aligned} \mathcal{I}(\psi) &= \int_{w < v} dv \int dw \int_{w' \geq v'} dv' \int dw' |v - w| \sigma(w', v' | w, v) \\ &\times \{ [\psi(v') - \psi(v)] \tilde{\rho}_2(r + s, w; r, v; t) \\ &+ [\psi(w') - \psi(w)] \tilde{\rho}_2(r, w; r - s, v; t) \}. \end{aligned} \quad (78)$$

Applying the Taylor approximation

$$\tilde{\rho}_2(r + s, w; r, v; t) \approx \tilde{\rho}_2(r, w; r - s, v; t) + s \frac{\partial}{\partial r} \tilde{\rho}_2(r + s, w; r, v; t) \quad (79)$$

yields

$$\mathcal{I}(\psi) = \mathcal{I}_s(\psi) - \frac{\partial \mathcal{I}_f(\psi)}{\partial r} \quad (80)$$

with the *source-like contribution*

$$\begin{aligned} \mathcal{I}_s(\psi) &= \int_{w < v} dv \int dw \int_{w' \geq v'} dv' \int dw' |v - w| \sigma(w', v' | w, v) \\ &\quad \times \{[\psi(v') + \psi(w')] - [\psi(v) + \psi(w)]\} \tilde{\rho}_2(r, w; r - s, v; t) \end{aligned} \quad (81)$$

and the *flux-like contribution*

$$\mathcal{I}_f(\psi) = -s \int_{w < v} dv \int dw \int_{w' \geq v'} dv' \int dw' |v - w| \sigma(w', v' | w, v) [\psi(v') - \psi(v)] \tilde{\rho}_2(r + s, w; r, v; t) \quad (82)$$

describing collisional transfer. In this representation we immediately see that the source-like contributions vanish for *collisional invariants* ψ , for which $\psi(v') + \psi(w') = \psi(v) + \psi(w)$ holds. As a consequence, we have only flux-like contributions to the velocity and variance equation for ordinary gases or fluids. However, in granular material the conservation of kinetic energy gets lost due to inelastic, dissipative interactions. Therefore, a source-like contribution is expected in the equation for the so-called *granular temperature* Θ (cf. Eq. (90)). Since momentum is conserved during granular collisions, these yield only a flux-like contribution to the velocity equation, which results in a corrected pressure relation (cf. Eq. (93)). Therefore, we have again a velocity equation of the form (2) with a density-independent equilibrium velocity $V_e = g/\gamma$. Consequently, the instability condition for the granular flow is given by Eq. (29), if we assume the validity of approximation (52). Due to $\partial V_e / \partial \rho = 0$, the stationary and homogeneous solution of the granular density and velocity equation is stable at all densities ρ_e . For this reason, the approximation (52) is not valid for granular flows, and we must apply Grad's method with $N \geq 2$. For $N = 2$ we obtain the Gaussian-shaped Maxwell-Boltzmann distribution

$$P(v; r, t) \approx \frac{1}{\sqrt{2\pi\Theta}} \exp \left[-\frac{(v - V)^2}{2\Theta} \right], \quad (83)$$

because $\langle 1 \rangle \stackrel{!}{=} 1$, $\langle v \rangle \stackrel{!}{=} V$, and $\langle (v - V)^2 \rangle \stackrel{!}{=} \Theta$ imply $a_0(r, t) = 1$ and $a_1(r, t) = a_2(r, t) = 0$.

The explicit calculation of the interaction terms $\mathcal{I}(\psi)$ now calls for a specification of the differential cross section $\sigma(w', v' | w, v)$ of granular collisions. Since both interacting grains have to be equivalently treated (isotropy condition), the collision law $v' = \mu v + \mu' w$ implies $w' = \mu w + \mu' v$. Due to momentum conservation ($v' + w' = v + w$) we must set $\mu' = (1 - \mu)$. Therefore, we find the relation

$$\sigma(w', v' | w, v) = \delta(v' - [\mu v + (1 - \mu)w]) \delta(w' - [\mu w + (1 - \mu)v]), \quad (84)$$

which is invariant with respect to interchanging the particles. μ is a characteristic parameter of the granular material. It is related to the amount of *energy dissipation* because of

$$(v'^2 + w'^2) = (v^2 + w^2) - 2\mu(1 - \mu)(v - w)^2. \quad (85)$$

Since collisional energy must not be produced during the interactions, we find $0 \leq \mu \leq 1$. Moreover, since we have $v > w$ before the collision and $v' \leq w'$ after the collision, we obtain the further restriction $\mu \leq 1/2$. For $\mu = 0$ we have completely elastic collisions with an interchange of particle velocities, so that the interaction terms in the macroscopic equations (75) and (76) vanish in the limit $s \ll 1/\rho$ (like for ordinary gases or fluids). However, due to its analogy with vehicular traffic, we will focus on the extremely inelastic case $\mu = 1/2$ in which both particles have the same velocity after their collision.

Next, we will specify the pair distribution function $\tilde{\rho}_2$ of interacting grains. This is usually expressed by their one-particle phase-space densities $\tilde{\rho}$ in the following way [13]:

$$\tilde{\rho}_2(r + s, w; r, v; t) = \chi(r + s/2, t)\tilde{\rho}(r + s, w, t)\tilde{\rho}(r, v, t). \quad (86)$$

The factor

$$\chi(r + s/2, t) := \frac{1}{1 - \rho(r + s/2, t)s} \quad (87)$$

reflects the increase of the particle interaction rate [34] because the grains are extended by an amount $s/2$ around their centers, so that they collide earlier. A first-order Taylor approximation of $\tilde{\rho}_2$ gives

$$\begin{aligned} \chi(r \pm s/2, t)\tilde{\rho}(r \pm s, w, t)\tilde{\rho}(r, v, t) &\approx \chi(r, t)\tilde{\rho}(r, w, t)\tilde{\rho}(r, v, t) \\ &\times \left\{ 1 \pm \frac{s}{2\chi} \frac{\partial \chi}{\partial r} \pm s \left[\frac{1}{\rho} \frac{\partial \rho}{\partial r} + \frac{v - V}{\Theta} \frac{\partial V}{\partial r} + \frac{1}{2\Theta} \left(\frac{(v - V)^2}{\Theta} - 1 \right) \frac{\partial \Theta}{\partial r} \right] \right\}. \end{aligned} \quad (88)$$

With this, evaluating the interaction terms $\mathcal{I}(\psi)$ and neglecting higher order derivatives as well as products of derivatives (i.e. neglecting Navier-Stokes and Burnett corrections) finally yields the continuity equation and the following Euler-like equations for granular flows:

$$\frac{\partial V}{\partial t} + V \frac{\partial V}{\partial r} = -\frac{1}{\rho} \frac{\partial}{\partial r} (\mathcal{P} + \mathcal{P}_{\text{corr}}) + (g - \gamma V), \quad (89)$$

$$\frac{\partial \Theta}{\partial t} + V \frac{\partial \Theta}{\partial r} = -\frac{2}{\rho} [\mathcal{P} + (1 + 3\mu)\mathcal{P}_{\text{corr}}] \frac{\partial V}{\partial r} + 2\gamma(\Theta_0 - \Theta) - \mu(1 - \mu) \frac{8}{\sqrt{\pi}} \frac{\rho \Theta^{3/2}}{1 - \rho s}. \quad (90)$$

That is, in the velocity equation (89) the interaction term yields an additional contribution

$$\mathcal{P}_{\text{corr}} = (1 - \mu)\mathcal{P}\frac{\rho s}{1 - \rho s} \quad (91)$$

to the pressure. This diverges in the limit $\rho \rightarrow \rho_{\text{max}} = 1/s$ of extreme densities, whereas $\mathcal{P} = \rho\Theta$ vanishes, since the equilibrium variance $\Theta_e(\rho)$ given by the implicit equation

$$\Theta_e(\rho) = \Theta_0 - \mu(1 - \mu)\frac{4}{\gamma\sqrt{\pi}}\frac{\rho\Theta_e^{3/2}(\rho)}{1 - \rho s} \quad (92)$$

vanishes. In the elastic case $\mu = 0$ we obtain the formula of van der Waals for the *total pressure* \mathcal{P}_{tot} in a gas of hard spheres:

$$\mathcal{P}_{\text{tot}} := \mathcal{P} + \mathcal{P}_{\text{corr}} = \mathcal{P} \left(1 + (1 - \mu)\frac{\rho s}{1 - \rho s} \right) \stackrel{\mu=0}{=} \frac{\mathcal{P}}{1 - \rho s}. \quad (93)$$

The last term in the variance equation (90) results from energy dissipation during granular collisions. Moreover, we have discovered a new contribution $3\mu\mathcal{P}_{\text{corr}}$ to the pressure, which (to the knowledge of the author) has not been reported elsewhere, presumably because it only plays a role in very inelastic cases ($\mu \not\approx 0$).

A linear stability analysis about the stationary and spatially homogeneous solution of Eqs. (74), (89), and (90) leads to the characteristic polynomial

$$\begin{aligned} & -\tilde{\lambda}^3 + \tilde{\lambda}^2 \left(2\frac{\partial\Theta_e}{\partial\Theta} - 3 \right) \gamma + \tilde{\lambda} \left\{ 2\gamma^2 \left(\frac{\partial\Theta_e}{\partial\Theta} - 1 \right) \right. \\ & \quad \left. - k^2 \left[\frac{\partial\mathcal{P}_{\text{tot}}}{\partial\rho} + \frac{2}{(\rho_e)^2} (\mathcal{P}_{\text{tot}} + 3\mu\mathcal{P}_{\text{corr}}) \frac{\partial\mathcal{P}_{\text{tot}}}{\partial\Theta} \right] \right\} \\ & - 2\gamma k^2 \left[\frac{\partial\mathcal{P}_{\text{tot}}}{\partial\rho} \left(1 - \frac{\partial\Theta_e}{\partial\Theta} \right) + \frac{\partial\mathcal{P}_{\text{tot}}}{\partial\Theta} \frac{\partial\Theta_e}{\partial\rho} \right] \stackrel{!}{=} 0. \end{aligned} \quad (94)$$

Its numerical investigation shows that the Euler-like equations for granular flows are unstable if the *noise level* Θ_0 is sufficiently large (cf. Fig. 9). The mechanism of the clustering instability originates from the increase of granular pressure with growing density. This causes a reduction of velocity (cf. Eq. (89)) which results in a further compression (cf. Eq. (74)). Since Eq. (94) implies

$$\tilde{\lambda}(\rho_e, k) = \tilde{\lambda}(\rho_e, -k) \quad \text{and} \quad \tilde{\omega}(\rho_e, k) = \tilde{\omega}(\rho_e, -k), \quad (95)$$

the *relative propagation speed*

$$u(\rho_e, k) := \frac{\tilde{\omega}(\rho_e, k)}{k} = -\frac{\tilde{\omega}(\rho_e, -k)}{-k} = -u(\rho_e, -k) \quad (96)$$

and the *relative group velocity*

$$c(\rho_e, k) := \frac{\partial\tilde{\omega}(\rho_e, k)}{\partial k} = -\frac{\partial\tilde{\omega}(\rho_e, -k)}{\partial(-k)} = -c(\rho_e, -k) \quad (97)$$

of perturbations with respect to V_e are *antisymmetric* functions in k . This is in contrast to the situation for vehicular traffic (cf. Fig. 12b).

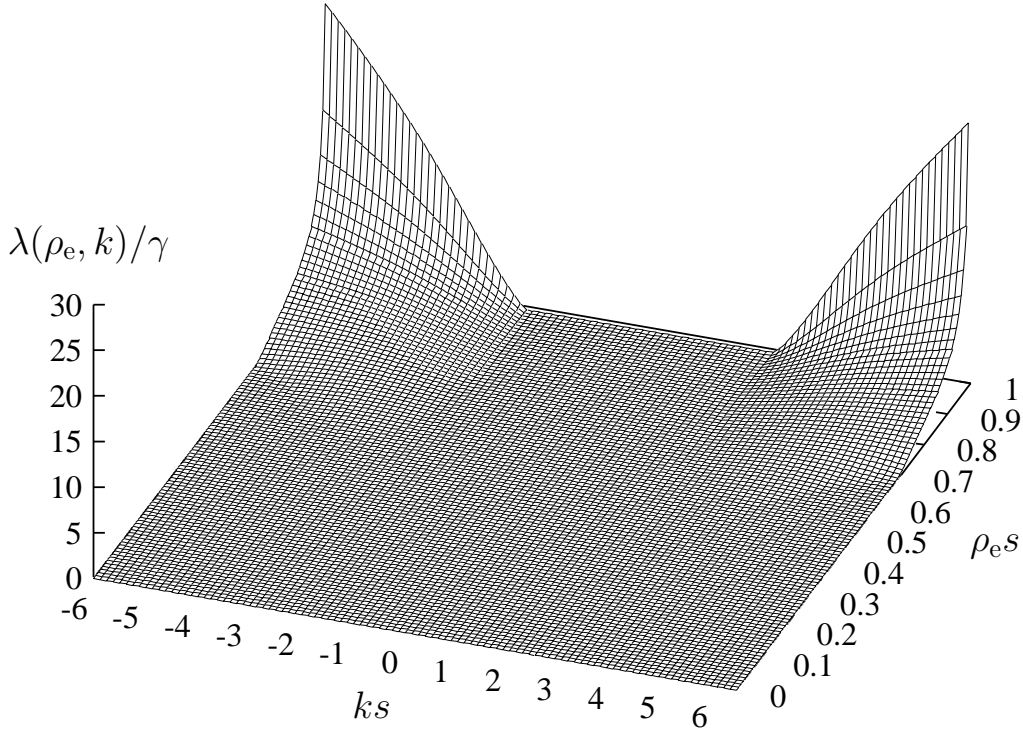


Figure 9: Illustration of the largest growth parameter λ in units of γ for the instability region (i.e. where $\lambda(\rho_e, k)/\gamma \geq 0$). The wave numbers in units of $1/s$ are restricted to the range $-2\pi \leq ks \leq 2\pi$, since wave lengths shorter than the diameter s of the grains cannot be propagated by the granular material. Granular flow is stable for wave numbers $k \approx 0$. Emergent density waves appear above a density-dependent critical value of $|k|$. These develop faster with growing absolute wave numbers $|k|$ and increasing densities ρ_e . A smaller degree of dissipation μ (here: $\mu = 1/2$) results in an expansion of the instability region towards higher densities ρ_e and smaller absolute wave numbers $|k|$. Decreasing the noise level Θ_0 leads to a reduction of the instability region, until it vanishes below a certain critical value.

5.2 Traffic flow

Our previously discussed traffic model is now very easily extended to the description of dense traffic. Again, we can apply formula (78). However, inserting (61) shows that the last term, which corresponds to backward interactions, vanishes. Therefore, the only difference between (62) and (78) is the replacement of $\rho^2 P(v; r, t) P(w; r, t)$ by the pair distribution function $\tilde{\rho}_2(r + s, w; r, v; t)$. In addition, we must take into account that vehicles require a *velocity*-dependent space of about

$$s(V) := \frac{1}{\rho_{\max}} + TV, \quad (98)$$

since drivers keep on average a *save distance* of length TV , where $T \approx 0.8$ s is about the *reaction time*. As a consequence, we get the modified relation

$$\tilde{\rho}_2(r + s, w; r, v; t) = \chi(r + TV, t) \rho(r + s(V), t) P(w; r + s(V), t) \rho(r, t) P(v; r, t) \quad (99)$$

with

$$\chi(r + TV, t) = \frac{1}{1 - \rho(r + TV, t) s(V)}. \quad (100)$$

$r + TV(r, t)$ is the *interaction point* of a vehicle at place r with a vehicle at place $r + s(V(r, t))$. In contrast to our discussion of grains, r and $r + s(V)$ are not the centers but the fronts of the vehicles.

Now, we can evaluate the collision terms (78). Applying Taylor approximations for $\chi(r + TV, t)$ and $\tilde{\rho}(r + s(V), w, t)$, we finally obtain the velocity equation

$$\frac{\partial V}{\partial t} + V \frac{\partial V}{\partial r} = -a_1 \frac{\partial \rho}{\partial r} + a_2 \frac{\partial V}{\partial r} - a_3 \frac{\partial \Theta}{\partial r} - b_1 \frac{\partial^2 \rho}{\partial r^2} + b_2 \frac{\partial^2 V}{\partial r^2} - b_3 \frac{\partial^2 \Theta}{\partial r^2} + \frac{1}{\tau} (V_e - V). \quad (101)$$

We have neglected products of partial derivatives (Burnett corrections), but taken into account second order derivatives (Navier-Stokes terms). The abbreviations used in the

above equation are:

$$\begin{aligned}
a_1 &= \frac{\Theta}{\rho} + (1-p)\rho \left(\frac{s\chi}{\rho} + TV \frac{\partial\chi}{\partial\rho} \right) \left[\Theta \left(1 - \frac{\beta}{2} \right) + \beta V \sqrt{\frac{\Theta}{\pi}} \right], \\
a_2 &= (1-p)\rho \left\{ s\chi \left[\left(2 - \frac{3}{2}\beta \right) \sqrt{\frac{\Theta}{\pi}} + \frac{\beta}{2}V \right] - TV \frac{\partial\chi}{\partial V} \left[\Theta \left(1 - \frac{\beta}{2} \right) + \beta V \sqrt{\frac{\Theta}{\pi}} \right] \right\}, \\
a_3 &= 1 + (1-p)\rho s\chi \left(\frac{1-\beta}{2} + \frac{\beta V}{4\sqrt{\pi\Theta}} \right) \\
b_1 &= (1-p)\rho \left(\frac{s^2\chi}{2\rho} + \frac{(TV)^2}{2} \frac{\partial\chi}{\partial\rho} \right) \left[\Theta \left(1 - \frac{\beta}{2} \right) + \beta V \sqrt{\frac{\Theta}{\pi}} \right], \\
b_2 &= (1-p)\rho \left\{ \frac{s^2\chi}{2} \left[\left(2 - \frac{3}{2}\beta \right) \sqrt{\frac{\Theta}{\pi}} + \frac{\beta}{2}V \right] - \frac{(TV)^2}{2} \frac{\partial\chi}{\partial V} \left[\Theta \left(1 - \frac{\beta}{2} \right) + \beta V \sqrt{\frac{\Theta}{\pi}} \right] \right\}, \\
b_3 &= (1-p)\rho \frac{s^2\chi}{2} \left(\frac{1-\beta}{2} + \frac{\beta V}{4\sqrt{\pi\Theta}} \right), \tag{102}
\end{aligned}$$

and

$$V_e = V_0 - (1-p)\tau\rho\chi \left[\Theta \left(1 - \frac{\beta}{2} \right) + \beta V \sqrt{\frac{\Theta}{\pi}} \right]. \tag{103}$$

Again, we will eliminate the variance equation by means of the approximation $\Theta(r, t) \approx \Theta_e(\rho(r, t), V(r, t))$. In the case $\mathcal{C}_e \approx 0$ related to a speed limit, the *equilibrium variance* $\Theta_e(\rho, V)$ is given by the implicit equation

$$\Theta_e(\rho, V) = \alpha(V^2 + \Theta_e) + \frac{\tau}{2}(1-p)\rho\chi \left(\beta V \Theta_e + 2\beta^2 V^2 \sqrt{\frac{\Theta_e}{\pi}} \right), \tag{104}$$

which is obtained by evaluation of the variance equation. Consequently, Θ_e vanishes when V becomes zero, which is required for consistency [2, 6]. Applying the above approximation for the variance and again neglecting products of partial derivatives (i.e. Burnett corrections), we find

$$\frac{\partial V}{\partial t} + V \frac{\partial V}{\partial r} = -\frac{1}{\rho} \frac{\partial \mathcal{P}_{\text{tot}}}{\partial \rho} \frac{\partial \rho}{\partial r} + a \frac{\partial V}{\partial r} - b \frac{\partial^2 \rho}{\partial r^2} + \frac{\eta}{\rho} \frac{\partial^2 V}{\partial r^2} + \frac{1}{\tau}(V_e - V), \tag{105}$$

where

$$\begin{aligned}
\frac{\partial \mathcal{P}_{\text{tot}}}{\partial \rho} &:= \rho \left(a_1 + a_3 \frac{\partial \Theta_e}{\partial \rho} \right), \\
\eta &:= \rho \left(b_2 - b_3 \frac{\partial \Theta_e}{\partial V} \right) \\
a &:= a_2 - a_3 \frac{\partial \Theta_e}{\partial V}, \\
b &:= b_1 + b_3 \frac{\partial \Theta_e}{\partial \rho}, \tag{106}
\end{aligned}$$

and V_e are functions of ρ and V .

It is obvious that the loss of momentum conservation and the velocity-dependence of the vehicular space requirements have drastically changed the structure of the velocity equation: The terms containing a and b are completely new compared to the Navier-Stokes equation for ordinary or granular fluids [13] and compared to all previous macroscopic traffic models (cf. Sec. 2). Fortunately, the model solves the problems which were mentioned in Section 1:

- The variation of individual vehicle velocities is taken into account by the variance $\Theta_e(\rho, V)$.
- The equilibrium velocity V_e and the equilibrium variance Θ_e are monotonously decreasing functions that vanish at the finite density ρ_{\max} .
- The equilibrium variance $\Theta_e(\rho, V)$ vanishes when $V(r, t) = 0$.
- In equilibrium (i.e. for $\rho(r, t) = \rho_e$ and $V(r, t) = V_e(\rho_e)$) the density-gradient $\partial\mathcal{P}/\partial\rho$ of the total traffic pressure \mathcal{P} is non-negative, so that the latter is a monotonously increasing function of ρ_e (cf. Fig. 10). The singularity of the pressure at $\rho = \rho_{\max}$ guarantees that the upper bound $\rho_{\max} < \rho_{\text{bb}}$ cannot be exceeded by the density $\rho(r, t)$.
- We were able to explain viscosity as an effect of the finite distance $s(V)$ between interacting vehicles. Moreover, we obtained a theoretical expression for the viscosity $\eta(\rho, V)$, which not only depends on the density, but also on the mean velocity. In equilibrium $\rho(r, t) = \rho_e$, $V(r, t) = V_e(\rho_e)$, the viscosity is non-negative. The singularity of viscosity at $\rho = \rho_{\max}$ causes that extreme changes of $V(r, t)$ and $\rho(r, t)$ are smoothed out, so that the shock-formation problem is solved.
- The fluid-dynamic traffic model (43), (105) is able to describe the emergence of stop-and-go traffic at medium densities (cf. Fig. 12a). A linear stability analysis leads to the characteristic polynomial

$$\tilde{\lambda}^2 + \tilde{\lambda} \left(\frac{\eta k^2}{\rho_e} + \frac{1}{\tau} - ika - \frac{1}{\tau} \frac{\partial V_e}{\partial V} \right) + ik\rho_e \left(-\frac{ik}{\rho_e} \frac{\partial \mathcal{P}_{\text{tot}}}{\partial \rho} + \frac{1}{\tau} \frac{\partial V_e}{\partial \rho} + bk^2 \right) \stackrel{!}{=} 0. \quad (107)$$

The transition from stability to instability occurs on the condition

$$\rho_e \left| \frac{\partial V_e}{\partial \rho} \right| = b\rho_e \tau k^2 + \left(1 + \left| \frac{\partial V_e}{\partial V} \right| + \frac{\eta \tau k^2}{\rho} \right) \left(\frac{a}{2} \pm \sqrt{\frac{a^2}{4} + \frac{\partial \mathcal{P}_{\text{tot}}}{\partial \rho}} \right). \quad (108)$$

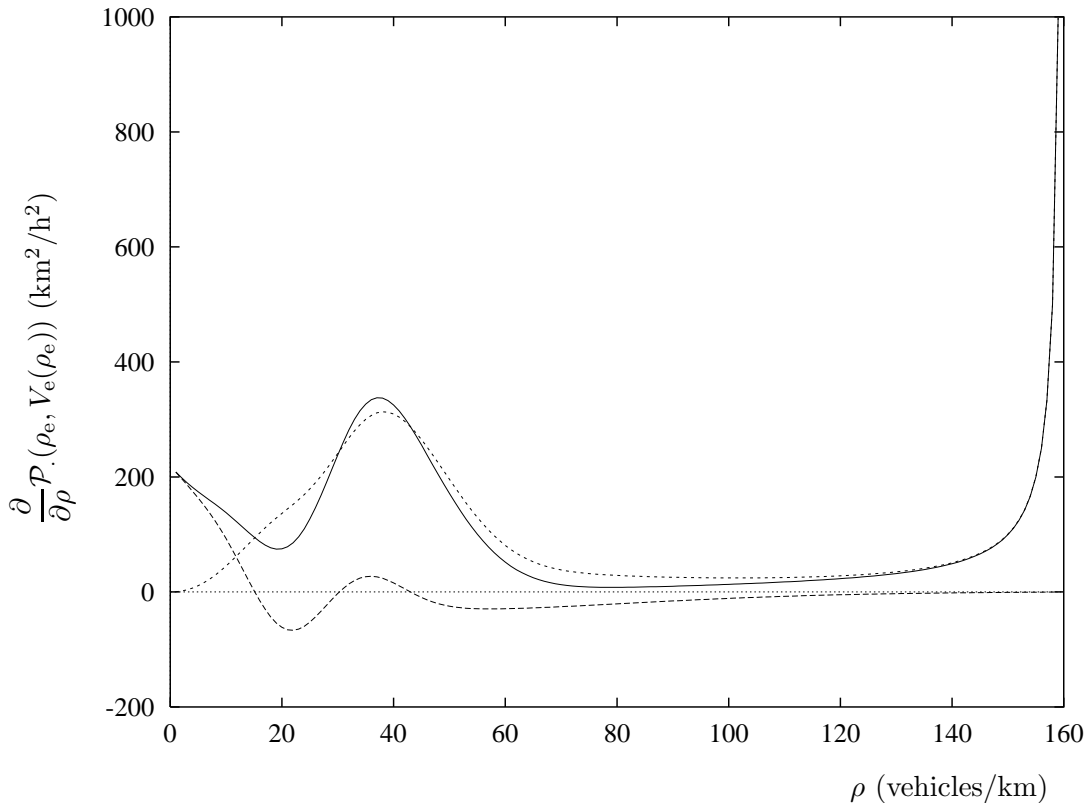


Figure 10: Comparison of the density-gradients of the total traffic pressure \mathcal{P}_{tot} (—), the idealized pressure $\mathcal{P} = \rho\Theta$ of point-like objects (---), and the correction term $\mathcal{P}_{\text{corr}}$ (- - -), estimated from empirical data. For $\rho \approx 20$ veh/km and large densities, the idealized traffic pressure \mathcal{P} of point-like objects decreases with growing density. However, this is more than compensated by the pressure correction $\mathcal{P}_{\text{corr}}$ due to the finite space requirements of vehicles. In particular, the increase of pressure with growing density diverges in the limit $\rho \rightarrow \rho_{\text{max}}$.

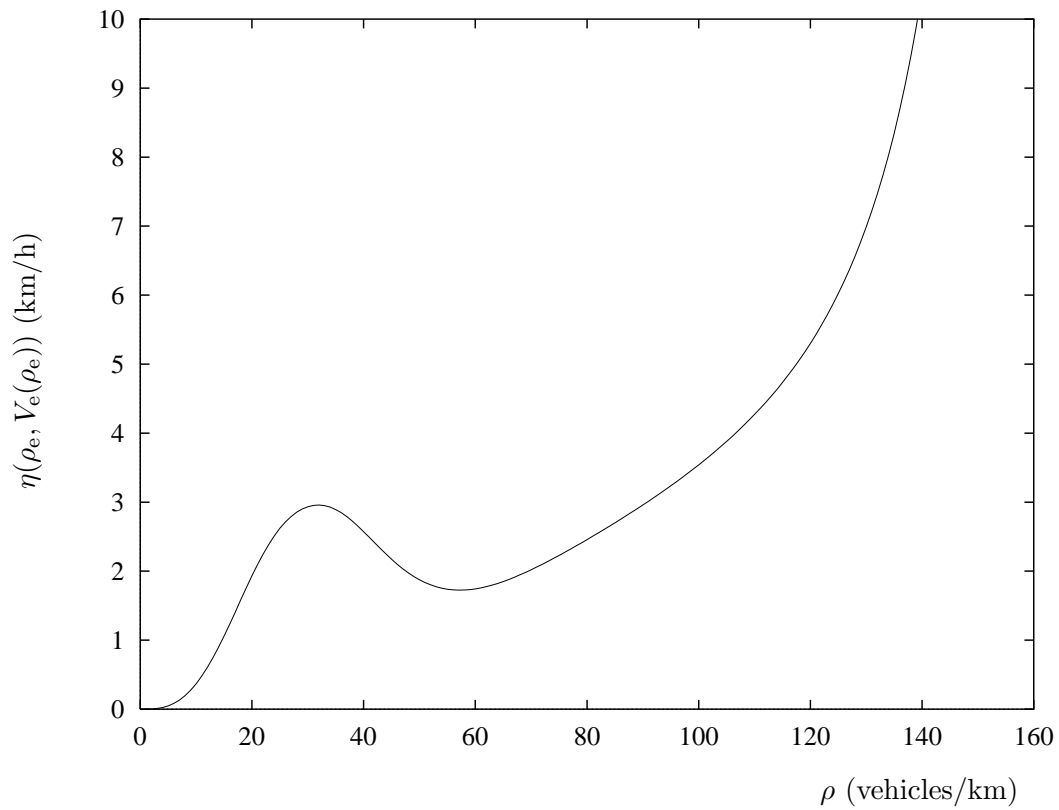


Figure 11: Illustration of the viscosity function estimated from empirical data. Obviously, the viscosity is non-negative, as expected, and diverges at large densities. Viscosity causes the smoothing effect which is necessary to avoid shock-like structures and to facilitate numerical simulations of the macroscopic traffic equations.

In contrast to Eq. (29), an additional instability appears at large absolute wave numbers $|k| > 130/\text{km}$. However, these are connected with wavelengths that are smaller than the average vehicle distance $1/\rho$ so that they cannot be propagated by the discontinuous vehicular fluid. Perturbations which can actually be propagated by the vehicles are moving in backward direction with respect to V_e (cf. Fig. 12b).

6 Summary and Outlook

It was shown that almost all macroscopic traffic models can be viewed as special cases of the continuity equation and a certain velocity equation. Although these equations have a close similarity to the hydrodynamic equations for ordinary fluids, they did not fulfill all consistency requirements for realistic traffic flow models.

Finally, it turned out that the correct structure of fluid-dynamic traffic equations looks considerably different. We obtained this result from a refined version of Paveri-Fontana's gas-kinetic traffic equation which was extended by the effects of imperfect driving and vehicular space requirements. In particular, we have applied the gas-kinetic theory of dense gases and granular materials.

Nevertheless, despite the phenomenologically similar behavior of traffic flow and granular material falling through a narrow vertical pipe, the governing equations and instability mechanisms are completely different. This was illustrated by numerical results of linear instability analyses and originates from the fact that momentum is conserved by granular collisions but not by vehicular interactions.

The parameters and relations occurring in the final model have been estimated from empirical traffic data. In addition, we have empirically tested the approximations that we made during the derivation of the fluid-dynamic traffic model. Finally, it was shown that all consistency criteria are met.

Future work will compare simulation results of the various discussed traffic models. Moreover, the refined traffic flow model (which treats the highway lanes in an overall manner) will be extended to a model for the different interacting highway lanes.

Acknowledgments

The author is very grateful to H. Taale and the Dutch Ministry of Transport, Public Works and Water Management for supplying the empirical traffic data. He also wants to

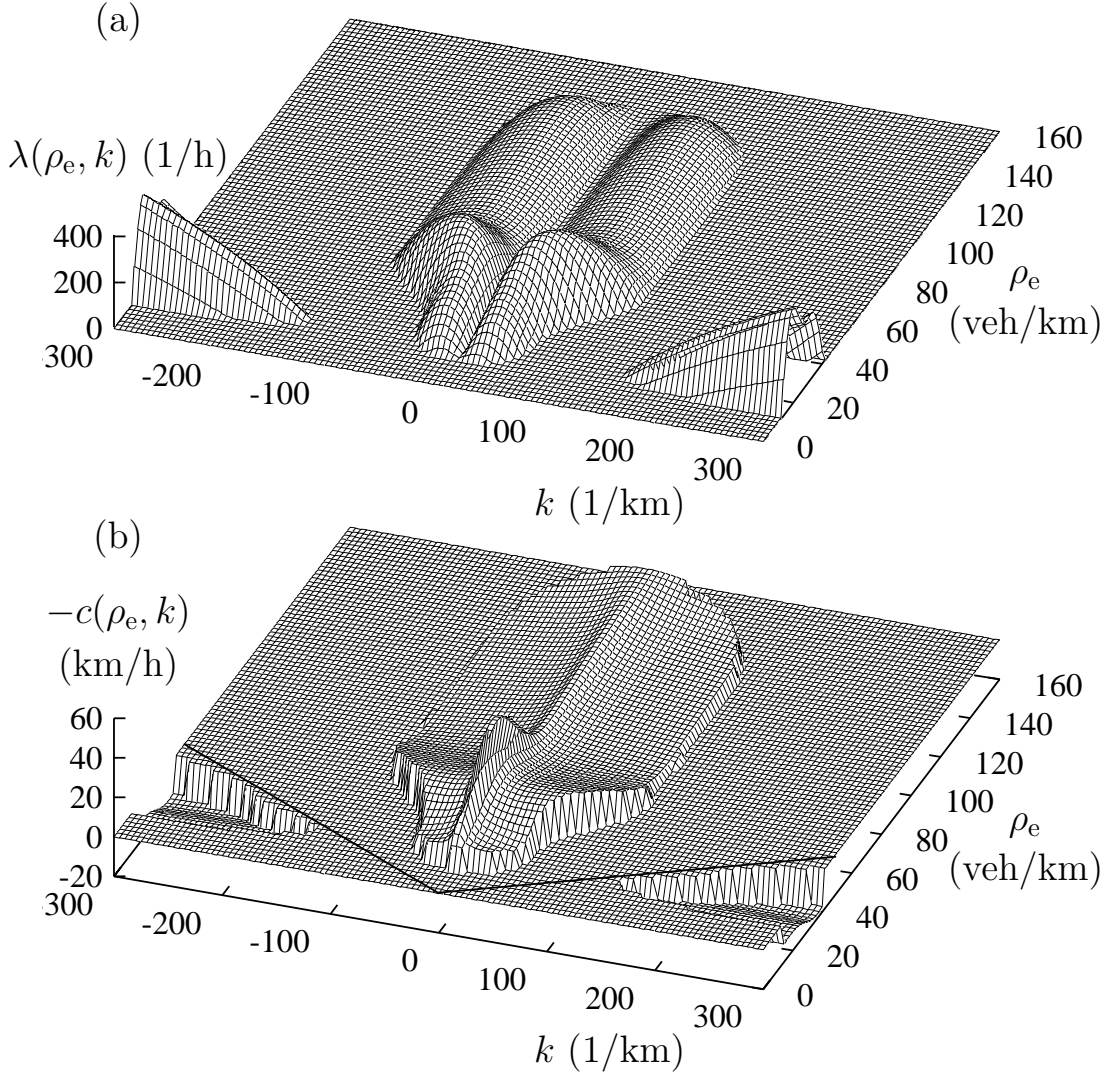


Figure 12: (a) Illustration of the largest growth parameter λ for the instability region of traffic flow (i.e. where $\lambda(\rho_e, k) \geq 0$). In contrast to granular flow (cf. Fig. 9), density waves develop at medium densities ρ_e and small absolute wave numbers $|k| \neq 0$. At moderate densities, the absolute wave number related to the largest growth rate increases with density, corresponding to a decrease of the wave length of forming stop-and-go waves. As expected, traffic flow is only stable at low densities (free flow) and extreme densities (slow-moving traffic). The instabilities for large absolute wave numbers $|k| > 130/km$ would be connected with stop-and-go waves that move in forward direction with group velocity $c(\rho_e, k) > 0$ relative to $V_e(\rho_e)$ (b). However, these instabilities are physically irrelevant, since they lie in front of the lines $\pm 2\pi\rho_e$ which characterize the maximum wave numbers that can be propagated by vehicles with an average distance of $1/\rho_e$ (= minimum wave length). The relevant instabilities at small absolute wave numbers $|k| < 2\pi\rho_e$ are connected with stop-and-go waves that move in backward direction with group velocity $|c(\rho_e, k)| > 0$ relative to $V_e(\rho_e)$. In contrast to Fig. 4, the propagation speed has the right

thank I. Goldhirsch, L. Schimansky-Geier, D. Rosenkranz, M. Hilliges, V. Shvetsov, and R. Kühne for inspiring discussions.

References

- [1] M. Cremer and J. Ludwig, *Math. Comput. Simulation* **28**, 297 (1986). K. Nagel and M. Schreckenberg, *J. Phys. I France* **2**, 2221 (1992). K. Nagel and H. J. Herrmann, *Physica A* **199**, 254 (1993). K. Nagel and A. Schleicher, *Parallel Computing* **20**, 125 (1994). K. Nagel and S. Rasmussen, in *Proceedings of the Alife 4 Meeting*, ed. R. Brooks and P. Maes (MIT press, Cambridge, MA, 1994). K. Nagel and M. Paczuski, *Phys. Rev. E* **51**, 2909 (1995). M. Schreckenberg, A. Schadschneider, K. Nagel, and N. Ito, *Phys. Rev. E* **51**, 2939 (1995). M. Bando, K. Hasebe, A. Nakayama, A. Shibata, and Y. Sugiyama, *Jpn. J. Ind. Appl. Math.* **11**, 203 (1994); *Phys. Rev. E* **51**, 1035 (1995).
- [2] D. Helbing, *Phys. Rev. E* **51**, 3164 (1995); in *Modelling and Simulation 1995*, ed. M. Snorek, M. Sujansky, and A. Verbraeck (The Society for Computer Simulation International, Istanbul, 1995).
- [3] M. Hilliges, R. Reiner, and W. Weidlich, in *Modelling and Simulation 1993*, ed. A. Pave (Society for Computer Simulation International, Ghent, Belgium, 1993). M. Hilliges and W. Weidlich, *Transpn. Res. B* **29**, 407 (1995). M. Hilliges, *Ein phänomenologisches Modell des dynamischen Verkehrsflusses in Schnellstraßennetzen* (Shaker, Aachen, 1995).
- [4] R. D. Kühne, in *Proceedings of the 9th International Symposium on Transportation and Traffic Theory*, ed. I. Volmuller and R. Hamerslag (VNU Science Press, Utrecht, The Netherlands, 1984); in *Proceedings of the 10th International Symposium on Transportation and Traffic Theory*, ed. N. H. Gartner and N. H. M. Wilson (Elsevier, New York, 1987). R. D. Kühne and M. B. Rödigier, in *Proceedings of the 1991 Winter Simulation Conference*, ed. B. L. Nelson, W. D. Kelton and G. M. Clark (Society for Computer Simulation International, San Diego, CA, 1991).
- [5] B. S. Kerner and P. Konhäuser, *Phys. Rev. E* **48**, 2335 (1993); *Phys. Rev. E* **50**, 54 (1994). B. S. Kerner, P. Konhäuser, and M. Schilke, *Phys. Rev. E* **51**, 6243 (1995).
- [6] D. Helbing, *Physica A* **219**, 375 (1995); *Physica A* **219**, 391 (1995); *Phys. Rev. E* **53**, 2366 (1996).

- [7] P. Nelson, *Transp. Theor. Stat. Phys.* **24**, 383 (1995).
- [8] F. L. Hall, B. L. Allen, and M. A. Gunter, *Transpn. Res. A* **20**, 197 (1986). F. L. Hall, *Transpn. Res. A* **21**, 191 (1987).
- [9] D. Helbing, *Verkehrsdynamik. Neue physikalische Modellierungskonzepte* (Springer, Berlin, 1996).
- [10] R. D. Kühne and K. Langbein, “Optimierung der Parameter einer Linienbeeinflussungsanlage” (Steierwald Schönharting und Partner GmbH, Heßbrühlstr. 21c, D-70565 Stuttgart).
- [11] M. Cremer, *Der Verkehrsfluß auf Schnellstraßen* (Springer, Berlin, 1979).
- [12] C. F. Daganzo, *Transpn. Res. B* **29**, 277 (1995).
- [13] J. T. Jenkins and M. W. Richman, *Phys. Fluids* **28**, 3485 (1985). C. K. K. Lun, S. B. Savage, D. J. Jeffrey, and N. Chepurniy, *J. Fluid Mech.* **140**, 223 (1984). S. Chapman and T. G. Cowling, *The Mathematical Theory of Nonuniform Gases* (Cambridge University Press, Cambridge, 3rd ed., 1970).
- [14] M. J. Lighthill and G. B. Whitham, *Proc. Roy. Soc. of London A* **229**, 317 (1955). G. B. Whitham, *Linear and Nonlinear Waves* (Wiley, New York, 1974).
- [15] P. I. Richards, *Op. Res.* **4**, 42 (1956).
- [16] C. F. Daganzo, *Transpn. Res. B* **28**, 269 (1994); *Transpn. Res. B* **29**, 79 (1995); *Transpn. Res. B* **29**, 261 (1995).
- [17] H. J. Payne, in *Mathematical Models of Public Systems*, Vol. 1, ed. G. A. Bekey (Simulation Council, La Jolla, CA, 1971); *Transportation Research Record* **722**, 68 (1979); in *Research Directions in Computer Control of Urban Traffic Systems*, ed. W. S. Levine, E. Lieberman, and J. J. Fearnside (American Society of Civil Engineers, New York, 1979).
- [18] D. C. Gazis, R. Herman, and R. B. Potts, *Op. Res.* **7**, 499 (1959). G. F. Newell, *Op. Res.* **9**, 209 (1961). D. C. Gazis, R. Herman, and R. W. Rothery, *Op. Res.* **9**, 545 (1961).
- [19] M. Papageorgiou, *Applications of Automatic Control Concepts to Traffic Flow Modeling and Control* (Springer, Berlin, 1983).

- [20] M. Cremer, *Der Verkehrsfluß auf Schnellstraßen* (Springer, Berlin, 1979). M. Cremer and A. D. May, *An Extended Traffic Model for Freeway Control* (Research Report UCB-ITS-RR-85-7, Institute of Transportation Studies, University of California, Berkeley).
- [21] S. A. Smulders, *Modelling and Simulation of Freeway Traffic Flow* (Report OS-R8615, Centre for Mathematics and Computer Science, Amsterdam, 1986); in *Proceedings of the 10th International Symposium on Transportation and Traffic Theory*, ed. N. H. Gartner and N. H. M. Wilson (Elsevier, New York, 1987).
- [22] J. M. Burgers, *Adv. Appl. Mech.* **1**, 171 (1948). G. B. Whitham, *Linear and Non-linear Waves* (Wiley, New York, 1974).
- [23] W. F. Phillips, *Kinetic Model for Traffic Flow* (Report No. DOT/RSPD/DPB/50-77/17, National Technical Information Service, Springfield, Virginia 22161, 1977); *Transportation Planning and Technology* **5**, 131 (1979).
- [24] I. Prigogine and F. C. Andrews, *Op. Res.* **8**, 789 (1960). I. Prigogine, in *Theory of Traffic Flow*, ed. R. Herman (Elsevier, Amsterdam, 1961). I. Prigogine and R. Herman, *Kinetic Theory of Vehicular Traffic* (American Elsevier, New York, 1971).
- [25] S. L. Paveri-Fontana, *Transpn. Res.* **9**, 225 (1975).
- [26] We have omitted the adaptation term which was suggested in Ref. [6] since it will be irrelevant in the following discussion.
- [27] H. Grad, *Comm. Pure Appl. Math.* **2**, 331 (1949). J. T. Jenkins and M. W. Richman, *Arch. Rat. Mech. Anal.* **87**, 355 (1985).
- [28] V. Shvetsov, private communication.
- [29] T. Riethmüller, L. Schimansky-Geier, D. Rosenkranz, and T. Pöschel (preprint). N. Sela and I. Goldhirsch, *Phys. Fluids* **7**, 507 (1995). S. McNamara and W. R. Young, *Phys. Fluids A* **5**, 34 (1993).
- [30] H. Hayakawa, S. Yue, and D. C. Hong, *Phys. Rev. Lett.* **75**, 2328 (1995). Y. S. Du, H. Li, and L. P. Kadanoff, *Phys. Rev. Lett.* **74**, 1268 (1995). J. Lee, *Phys. Rev. E* **49**, 281 (1994). I. Goldhirsch and G. Zanetti, *Phys. Rev. Lett.* **70**, 1619 (1993).
- [31] V. Frette et al., *Nature* **379**, 49 (1996). H. M. Jaeger and S. R. Nagel, *Science* **255**, 1523 (1992). S. R. Nagel, *Rev. Mod. Phys.* **64**, 321 (1992). S. F. Shandarin and Y.

- B. Zeldovich, *Rev. Mod. Phys.* **61**, 185 (1989). K. L. Schick and A. A. Verveen, *Nature* **251**, 599 (1974).
- [32] H. J. Herrmann, in *3rd Granada Lectures in Computational Physics*, edited by P. L. Garrido and J. Marro (Springer, Heidelberg, 1995). T. Pöschel and H. J. Herrmann, *Europhys. Lett.* **29**, 123 (1995). M. Bourzutschky and J. Miller, *Phys. Rev. Lett.* **75**, 4154 and **74**, 2216 (1995). F. Melo, P. B. Umbanhowar, and H. L. Swinney, *Phys. Rev. Lett.* **75**, 3838 (1995). G. Baumann, I. M. Janosi, and D. E. Wolf, *Europhys. Lett.* **27**, 203 (1994). J. Gallas, H. J. Herrmann, and S. Sokolowski, *Phys. Rev. Lett.* **69**, 1371 (1992). H. M. Jaeger, C.-H. Liu and S. R. Nagel, *Phys. Rev. Lett.* **62**, 40 (1989).
- [33] T. Raafat, J. P. Hulin and H. J. Herrmann, *Phys. Rev. E* (to be published). G. Peng and H. J. Herrmann, *Phys. Rev. E* **49**, R1796 (1994). T. Pöschel, *J. Phys. I France* **4**, 499 (1994). G. W. Baxter, R. P. Behringer, T. Fagert, and G. A. Johnson, *Phys. Rev. Lett.* **62**, 2825 (1989).
- [34] L. Verlet and D. Levesque, *Molec. Phys.* **46**, 969 (1982).